82638

BATSE OBSERVATIONS ON ACCRETION POWERED PULSARS

A THESIS SUBMITTED TO
THE GRADUATE SCHOOL OF NATURAL AND APPLIED SCIENCES
OF
THE MIDDLE EAST TECHNICAL UNIVERSITY

BY

SITKI ÇAĞDAŞ İNAM

82638

IN PARTIAL FULFILLMENT OF THE REQUIREMENTS FOR THE DEGREE OF

MASTER OF SCIENCE

IN

THE DEPARTMENT OF PHYSICS

T.C. YÜKSEKÖĞRETİM KURULU
DOKÜMANTASYON MERKEZİ

DECEMBER 1998

Approval of the Graduate School of Natural and Applied Sciences.

Prof. Dr. Tayfur Öztürk
Director

I certify that this thesis satisfies all the requirements as a thesis for the degree of Master of Science.

Prof. Dr. Sinan Bilikmen
Head of Department

This is to certify that we have read this thesis and that in our opinion it is fully adequate, in scope and quality, as a thesis for the degree of Master of Science.

Assoc. Prof. Dr. Altan Baykal
Supervisor

Examining Committee Members

Assoc. Prof. Dr. Altan Baykal

Prof. Dr. Ali Alpar

Prof. Dr. Oktay Hüseyin

Prof. Dr. Nilgün Kızıloğlu

Prof. Dr. Ümit Kızıloğlu

ABSTRACT

BATSE OBSERVATIONS ON ACCRETION POWERED PULSARS

İNAM, Sıtkı Çağdaş

M.S., Department of Physics

Supervisor: Assoc. Prof. Dr. Altan Baykal

December 1998, 88 pages.

In this thesis, analysis of BATSE 20-50keV flux and frequency data of 10 accretion powered pulsars (2S 1417-62, GS 0834-430, GRO J 1008-57, GRO J 1948+32, A 1118-616, Vela X-1, GX 301-2, OAO 1657-415, GX 1+4 and 4U 1626-67) is presented. Two transient sources (2S 1417-62 and GS 0834-430) are found to be torque and X-ray luminosity correlated implying the existence of prograde accretion disks. For these sources, errors are too big for the data to have preference on a single inner disk model. For high mass X-ray binaries (Vela X-1, GX 301-2 and OAO 1657-415), no correlation is found between torque and X-ray luminosity. These sources are found to be torque and specific angular momentum correlated. There is a possibility of temporary disk formation for these sources. For the low mass system GX 1+4, data is analyzed in four intervals. First part of the data gives torque and X-ray luminosity anticorrelation in spin-down implying a retrograde accretion disk. In the second part of the data, correlation of torque and X-ray luminosity is found in spin-up implying a prograde accretion disk. For the last two intervals, no correlation is found between X-ray luminosity and flux. For the other low mass system 4U 1626-67, a correlation of torque and X-ray luminosity is found in spin-down, which may be the indication of a prograde disk with dominating spin-down magnetic torques.

Keywords: Accretion powered pulsars, neutron stars, accretion disks, BATSE observations.

ÖZ

AKTARIM GÜÇLÜ ATARCALARIN BATSE GÖZLEMLERİ

İNAM, Sıtkı Çağdaş
Yüksek Lisans , Fizik Bölümü
Tez Yöneticisi: Assoc. Prof. Dr. Altan Baykal

Aralık 1998, 88 sayfa.

Bu tezde 10 aktarım güçlü atarcanın (2S 1417-62, GS 0834-430, GRO J 1008-57, GRO J 1948+32, A 1118-616, Vela X-1, GX 301-2, OAO 1657-415, GX 1+4 ve 4U 1626-67) BATSE 20-50keV akı ve frekans verilerinin analizi sunulmaktadır. İki geçici kaynakta (2S 1417-62 ve GS 0834-430) tork ve X-ışını parlaklığı arasında düz yönde dönen aktarım diski varlığını gösteren ilişki bulunmuştur. Bu kaynakların verilerindeki hataların büyüklüğü yüzünden iki kaynakta da tek bir iç disk modeline karar verilememiştir. Yüksek kütleli X-ışını çiftlerinde (Vela X-1, GX 301-2 ve OAO 1657-415) tork ve X-ışını parlaklığı arasında bir ilişki bulunamamıştır. Bu kaynakların verilerinde tork ve özgül açısal momentum arasında bir ilişki bulunmuştur. Bu kaynaklarda geçici aktarım diski oluşumunun mümkün olduğu düşünülmektedir. GX 1+4 verilerinin ilk kısmında tork ve X-ışını parlaklığı arasında atarca yavaşlarken aksi bir ilişki bulunmuştur. Bu ilişki ters dönen bir aktarım diskinin varlığını gösteriyor olabilir. Verilerin ikinci kısmında, tork ve X-ışını parlaklığı arasında atarca hızlanırken ilişki bulunmuştur. Bu ilişki düz dönen bir aktarım diskinin varlığına işaret olabilir. Verilerin son iki kısmında, tork ve X-ışını parlaklığı arasında bir ilişki bulunamamıştır. 4U 1626-67 kaynağının verilerinin analizi sonucunda, atarca yavaşlarken tork ve X-ışını

parlaklığı arasında bir ilişki bulunmuştur. Bu ilişki yavaşlatıcı manyetik torkların baskın olduğu düz dönen bir diskin göstergesi olabilir.

Anahtar Kelimeler: Aktarım güçlü atarcalar, nötron yıldızları, kütle aktarım diskleri, BATSE gözlemleri.

ACKNOWLEDGMENTS

I would like to express my deepest gratitude to Assoc. Prof. Dr. Altan Baykal for his guidance and insight throughout the research.

I would like to thank to Prof. Dr. Ali Alpar for his helpful discussions and useful suggestions.

I thank my friends and colleagues in METU Astrophysics Group and TÜBİTAK High Energy Astrophysics Unit for their support. I also thank my parents for their economical and moral support. I acknowledge a scholarship provided by Turkish Scientific Research Council (TÜBİTAK).

TABLE OF CONTENTS

LIST OF TABLES

LIST OF FIGURES

CHAPTER 1

INTRODUCTION

A neutron star is the end product of the evolution of a massive star. When the core of a star uses up the nuclear energy, radiation pressure can no longer balance the gravity. The core begins to collapse until degenerate electron pressure balances gravity. If the core mass is less than $\simeq 1.4M_{\odot}$, degenerate electrons can prevent the core from collapsing any more. The star becomes a white dwarf with a radius of about 10^9cm. If the mass of the core is $\simeq 1.4 - 2M_{\odot}$, degenerate electron pressure cannot stop the collapse of the core. Electrons and protons merge to form neutrons, and when the radius of the core reduces to $\simeq 10^6$cm, degenerate neutron pressure begins to support the core and thus a neutron star forms. For a core with mass greater than a limiting mass currently estimated to be $\simeq 2M_{\odot}$, no known force can prevent the collapse, and a black hole forms.

Neutron stars are perfect space laboratories to study extreme physical conditions that cannot be realized in a terrestrial laboratory. Neutron stars have macroscopic sizes, but -being degenerate stars- the properties of their interior structure can only be understood in terms of elementary particle physics and condensed matter physics. The physical conditions in the vicinity of a neutron star are also interesting. Neutron stars have very large surface dipole magnetic fields

T.C. YÜKSEKÖĞRETİM KURULU
DOKÜMANTASYON MERKEZİ

($\sim 10^9 - 10^{12}$ Gauss), and very strong gravitational fields ($g_{surface} \sim 10^{14}$cm.s^{-2}). These two factors determine the plasma flow around neutron stars and make neutron stars interesting objects for plasma physics as well.

If a neutron star is in a binary system with a non-degenerate companion,[1] mass flow from the companion to the neutron star may occur.

For a close binary system for which the companion star can overfill its Roche lobe, mass is transferred via the inner Lagrangian point and a Keplerian accretion disk forms in the vicinity of the neutron star. Mass is transferred through the disk onto the neutron star mainly from the inner boundary of the disk which is at a radius close to the magnetospheric radius of the neutron star. After leaving the inner boundary of the disk, mass follows the magnetic field lines to the polar regions of the neutron star.

If the system is a wide binary so that the companion cannot overfill its Roche lobe, there may still be mass transfer to the neutron star from the stellar wind originating from the companion's surface. For such a system, no stable disk formation is possible. There may be temporary accretion disk formation with a lifetime of the order of days in case of fast wind from an OB or Be type giant star, or of the order of years in case of slow wind from a red giant.

Plasma accreting onto the polar regions of the neutron star is heated due to the release of the gravitational potential energy of the plasma. Heated plasma radiates primarily in the X-ray band. In general the magnetic axis does not

[1] A neutron star is a product of a supernova explosion. If more than half of the mass of the binary system is ejected during the explosion, binary system will be separated.

coincide with the spin axis, so that the neutron star is like a lighthouse which pulses when one or two poles of it is/are on our line of sight. In other words, we expect to see X-ray pulsations from such a neutron star. Neutron stars of this type are called *accretion powered pulsars.* Accreted plasma also carries angular momentum to the neutron star so that the neutron star is exerted torque causing a change in the spin period. As the moment of inertia of the neutron star is much smaller than a non-degenerate star, we expect to observe changes in the spin period.

Observations of changes in X-ray flux of accretion powered pulsars is also important to analyze plasma flow near the neutron star. Change in X-ray flux is an indicator of the change in mass acretion rate and physical characteristics of plasma flow. Since plasma carries angular momentum to the neutron star, change in plasma accretion may change the torque exerted on the neutron star which can be seen by analyzing the changes in the frequency derivative found from the frequency history of the pulsar.

In this thesis, we use flux and frequency data from BATSE (Burst and Transient Source Experiment) detector in CGRO (Compton Gamma Ray Obsefvatory) satellite. BATSE continuously monitors the spin frequency and pulsed flux in 20-50 keV band of three low-mass systems (Her X-1, 4U 1626-67, GX 1+4), and five high mass systems (Cen X-3, OAO 1657-415, Vela X-1, 4U 1538-52, and GX 301-2). BATSE has also observed outbursts from 12 transients (4U 0115+63, GS 0834-430, 2S 1417-62, EXO 2030+375, A 0535+26, 4U 1145-619, A 1118-616, GRO J1744-28, GRO J1750-27, GRO J1948+32, GRO J1008-57, and GRO

J2058+42). In the thesis, data of 10 of these pulsars are analyzed, 2 of which are low-mass systems (GX 1+4, 4U 1626-67), 3 of which are high-mass systems (OAO 1657-415, Vela X-1, GX 301-2) and 5 of which are transients (GS 0834-430, 2S 1417-624, A 1118-616, GRO J1948+32, GRO J1008-57).

In the next chapter, overview of accretion powered pulsars is presented. Theories of torques on accretion powered pulsars are reviewed in Chapter 3. In Chapters 4,5 and 6, analysis of flux and frequency data is presented.

CHAPTER 2

OVERVIEW

Accretion powered pulsars are rotating, highly magnetized neutron stars which are capturing matter from a stellar companion. Due to the high dipole magnetic field, accreting matter is channeled by the magnetic field lines onto the magnetic poles of the neutron star. When the matter falls onto the neutron star, it is rapidly decelerated at the polar surface which causes the release of the gravitational potential energy as X-ray emission from the magnetic poles. Due to the fact that the magnetic axis is in general tilted with respect to the spin axis of the neutron star, we expect to see X-ray pulses from the neutron star.

Observations of accretion powered pulsars began with the discovery of periodic X-ray pulsations from Cen X-3 by *Uhuru* (Giaconni et al. 1971; Schreier et al. 1972). Qualitative understanding of accretion powered pulsars were achieved in 1970s (Pringle& Rees 1972; Davidson& Ostriker 1973; Lamb et al. 1973).

We can divide accretion powered pulsar systems into 3 groups according to their companions: 1. High mass X-ray binaries with OB supergiant companions, 2. low mass X-ray binaries, 3. Be-star X-ray binaries.

Pulsars in high mass X-ray binaries with OB supergiant companions accrete mass either via Roche lobe overflow or via the supergiant's stellar wind. Systems

with the first type of the pulsars have short pulse periods and high X-ray luminosities (SMC X-1 with the pulse period of 0.717s and luminosity of 6×10^{38}ergs.s^{-1}; Cen X-3 with the pulse period of 4.8s and luminosity of 8×10^{37}ergs.s^{-1}). Systems with the second type of the pulsars have long pulse periods and moderate X-ray luminosities (Vela X-1 with the pulse period of 283s and luminosity of 6×10^{36}ergs.s^{-1}) (Corbet, 1986; Chakrabarty 1996).

Low mass X-ray binaries have late type or degenerate dwarf companions. These systems are steady and low luminosity X-ray sources ($< 10^{37}$ergs.s^{-1}). GX 1+4 and 4U 1626-67 are typical examples.

Systems with Be-star companions constitute the third group. These systems contain rapidly rotating Be companions (4U 0115+63 and A 0535+62). These systems are transient X-ray sources which are X-ray bright near the periastron passage of an eccentric orbit.

For the high mass systems, we can roughly estimate type of the system by plotting spin period versus orbital period (*see* Figure 2.1). This figure is also known as Corbet diagram(Corbet 1986; Chakrabarty 1996). For disk-fed supergiant systems, we have short spin and orbital periods. Short orbital period for such a system is a sign of the possibility of the Roche-lobe overflow. Thus, a Keplerian accretion disk forms around the neutron star and spins-up the neutron star which explains the short spin periods. For the wind-fed supergiant systems, spin and orbital periods are larger. Large spin period shows large binary seperation and large Roche lobe of the companion, so it shows the impossibility of

Figure 2.1: Spin period versus orbital period for the accretion powered pulsars with high mass companions (Chakrabarty 1996).

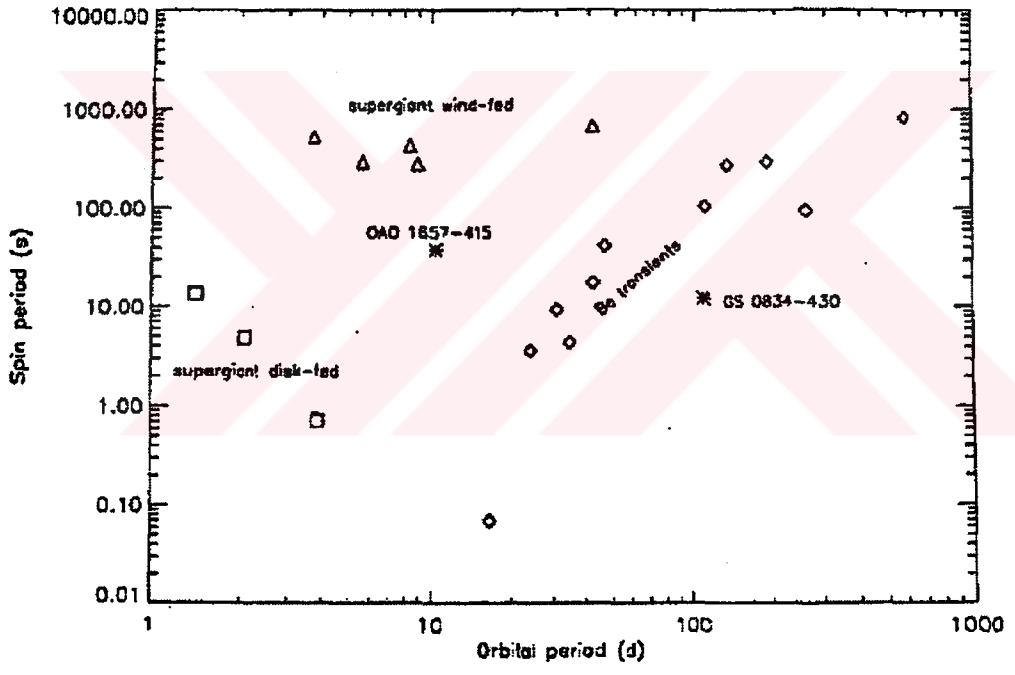

Figure 2.2: Distribution of accretion powered pulsars in galactic coordinates (Chakrabarty 1996).

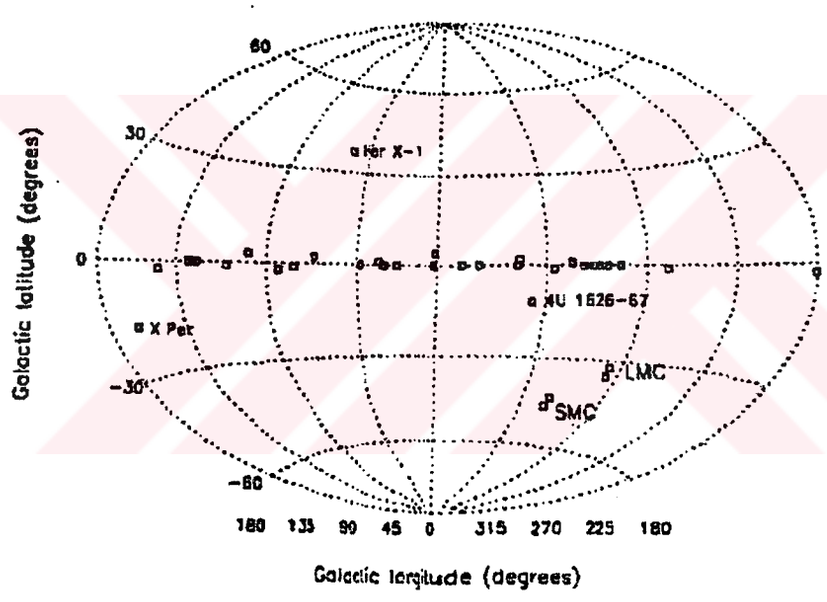

the Roche lobe overflow. This makes a stable accretion disk formation improbable. The pulsar accretes mass from the wind and no strong trend in the torque is expected which means that spin-up and spin-down torques should be similar in magnitude which excludes the possibility of a spin-up trend and that is why we do not observe short spin periods from these systems. For systems with Be-star companions a rough correlation between orbital period and spin period is observed (Corbet 1986; Waters& van Kerkwijk 1989).

About 40 accretion powered pulsars are known with pulse periods ranging from 0.069s to 23.5minutes (Chakrabarty 1996). Most of these pulsars lie in the galactic plane, a few are located in the magellanic clouds and a few are in the high-latitudes of our galaxy (*see* Figure 2.2).

To understand the nature of the plasma flow in the vicinity of an accretion powered pulsar, a direct method is to observe the changes in spin-period and corresponding changes in flux. Changes in spin period gives us the magnitude and direction of the torque exerted on the neutron star. This torque is carried by the accreted plasma so it depends on the specific angular momentum, the amount of the plasma and the accretion geometry. Frequency changes of an accretion powered pulsar and its relation with the changes in the X-ray flux of this pulsar offer us possibility to test the theories about accretion process in binaries with compact objects. Spin rate and changes in flux give us information about the process of accretion flow near the magnetosphere, and internal properties of neutron stars. So, for example, long-term period and flux changes give us information about the time averaged circulation of the accretion plasma, neutron

star's dipole magnetic field and the size of its moment of inertia, whereas short-term period fluctuations gives us an idea about the stability of the accretion flow and the internal dynamical properties of neutron stars.

Burst and Transient Source Experiment (BATSE) detectors in *Compton Gamma Ray Observatory* (CGRO) have the ability to continuously monitor the spin frequency and flux of accreting pulsars. Data obtained from BATSE observations enable us to understand the relation between the torque and X-ray luminosity changes.

In this thesis, analysis of BATSE observations of pulse frequency and flux from 20-50 keV band on 10 accretion powered pulsars (GX 1+4, 4U 1626-67, Vela X-1, OAO 1657-415, GX 301-2. 2S 1417-62. GS 0834-430, A 1118-616, GRO J1948+32, GRO J1008-57) is discussed. Data are the 20-50 keV X-ray flux and frequency of the pulsed flux data obtained from BATSE on the CGRO. These data are accessible at ftp area at ftp.cossc.gsfc.nasa.gov.

CHAPTER 3

THEORY OF TORQUES ON ACCRETION POWERED PULSARS

3.1 Introduction

An accretion powered pulsar is an accreting neutron star in a binary system which shows X-ray pulsations at its rotation(spin) period. The source of this X-ray luminosity is the gravitational potential energy release of the plasma originating from the companion star. This luminosity can approximately be written as

$$L \cong \frac{GM\,\dot{M}}{R} = 10^{36}\mathrm{erg.s}^{-1}\left[\frac{M}{1.4M_{\odot}}\right]\left[\frac{\dot{M}}{10^{-10}M_{\odot}\mathrm{yr}^{-1}}\right]\left[\frac{R}{10\mathrm{km}}\right]^{-1} \qquad (3.1)$$

where M and R are the mass and the radius of the neutron star, and $\dot{M}$ is the mass accretion rate.

Pulsations in the X-ray luminosity of the accretion powered pulsar are due to the anisotropy of the infalling plasma (infall is primarily to the magnetic polar regions because of the high dipolar magnetic field) and the angle between the spin axis and the magnetic dipole axis. Orbital motions of these pulsating systems have additional effects on the pulse profiles because of the eclipses and the Doppler

effect.

3.2 Preliminaries about Accretion on Neutron Stars

To understand the nature of accretion on neutron stars, firstly it must be emphasized that neutron stars have very large surface dipole magnetic fields ($\sim 10^9 - 10^{12}$Gauss, while the surface magnetic field of the Sun is about 1 Gauss, and that of the Earth is about 0.25 Gauss). Moreover, the strong gravitational field with a surface gravitational acceleration of about 10^{14}cm.s^{-2} (while $g_\odot \approx 10^4$cm.s^{-2} and $g_{Earth} \approx 10^3$cm.s^{-2}) due to neutron star's compact structure is also an important factor determining the physics of accretion. Finally, another effect on the accretion process is the one coming from the intense X-ray radiation from the neutron star, which may -in some cases- cause a radiation pressure force comparable to the gravitational force but in the opposite direction, inhibiting the accretion process.

Let us consider a newborn neutron star in a binary system emitting radio pulses and ejecting cosmic rays like a radio pulsar[1]. This operation of the neutron star is the consequence of the corotation of its dipolar electromagnetic field. In general, for a rotating magnetic dipole which is generally a reasonable approximation for neutron stars, we must also consider an induced electric component of the field due to the rotation. At a radius much smaller than the light cylinder radius(r_{cyl}) [2], electric field component ($\mathcal{E}$) of the electromagnetic field can be

[1] But in general, the free-free absorption in the surrounding plasma originating from the supernova explosion or coming from the companion star prevents pulses from being observed.

[2] around the spin axis of the neutron star beyond which the matter cannot corotate with

written as(Lipunov, 1992)

$$\mathcal{E} \simeq \frac{v}{c}\mathcal{B} = \frac{\Omega r}{c}\mathcal{B} = \frac{r}{r_{cyl}}\mathcal{B}, \tag{3.2}$$

where v is the linear velocity of the rotating field, c is the speed of light, Ω is the angular velocity of the neutron star and $\mathcal{B}$ is the magnetic component of the field at a radius r from the neutron star. For regions close to the neutron star where $r \ll r_{cyl}$, Equation (3.2) gives a very small electric field component.But as r approaches r_{cyl}, magnitude of the electric field strength approaches that of the magnetic field strength, and for $r \gg r_{cyl}$, the electromagnetic field becomes a freely propagating electromagnetic field for which $\mathcal{E} = \mathcal{B}$ This electromagnetic field formation is called the operation of the radio pulsar.

For the surrounding plasma to reach the surface of the neutron star, firstly the pressure of the plasma at the gravitational capture radius ($r_{capt} = \frac{GM}{v^2}$), which can be written as

$$\mathcal{P}_{plasma}(r = r_{capt}) = \rho v^2, \tag{3.3}$$

where ρ is the density of the plasma written as

$$\rho(r = r_{capt}) = \frac{\dot{M}}{4\pi r^2 v}, \tag{3.4}$$

for spherically symmetric accretion with v being the velocity of the plasma, should overcome the pressure of the electromagnetic field which can be expressed

the star. Radius of the light cylinder is given by $r_{cyl} = cP/2\pi$ where P is the spin period of the neutron star.

T.C. YÜKSEKÖĞRETİM KURULU
DOKÜMANTASYON MERKEZİ

as

$$\mathcal{P}_{\rm EM}(\mathrm{r} = \mathrm{r}_{\rm capt}) = \frac{\mathrm{L}}{4\pi \mathrm{r}^2 \mathrm{c}}. \tag{3.5}$$

where L is the luminosity of the neutron star due to its radio pulsar operation that can be written as

$$L = \frac{2}{3}\frac{\mu^2 (2\pi)^4}{P^4 c^3}, \tag{3.6}$$

P being the period and $\mu(\sim BR^3$, B: the surface magnetic field of the neutron star) being the magnetic moment of the neutron star.[3]Thus, equating the luminosity of the plasma ($L' = 4\pi r_{capt}^2 c\rho v^2 = 4\ \dot{M}\ vc$) and the luminosity of the neutron star at the gravitational capture radius, one can find a critical period above which the plasma can be captured by the gravity of the neutron star. This critical period is (Illarionov & Sunyaev 1975):

$$P_{cr} = \frac{2\pi}{c}\left[\frac{\mu^2}{6\ \dot{M}\ v}\right]^{1/4} \tag{3.7}$$

$$= 0.1\left[\frac{\mu}{10^{29}\mathrm{Gauss.cm}^3}\right]^{1/2}\left[\frac{\dot{M}}{1.5\times 10^{-11} M_\odot \mathrm{year}^{-1}}\right]^{-1/4}\left[\frac{v}{10^8 \mathrm{cm.s}^{-1}}\right]^{-1/4} \mathrm{s}$$

If initial period of the neutron star is $\geq$ 0.1s, which is not typical for newborn neutron stars, then the neutron star may capture plasma just after it has been formed. The deceleration time for spin-down from initial period to the critical period can be formulated as (Illarionov & Sunyaev 1975)

[3] $r_{capt} > r_{cyl}$.

$$t(P_{cr}) = \frac{I\left(\frac{2\pi}{P_{cr}}\right)^2}{2L(P_{cr})} = \frac{3c^3 I}{4\mu^2}\left(\frac{P_{cr}}{2\pi}\right)^2 = \frac{3cI}{4\mu\sqrt{6\,\dot{M}\,v}}s \tag{3.8}$$

where $I \simeq 10^{45}$g.cm^2 is the moment of inertia of the neutron star and L is the total luminosity which is proportional to $1/P^4$ (See Equation (3.6)). For $v = 10^8$cm.s^{-1}, $\mu = 10^{29}$Gauss.cm^3, and $\dot{M}$= $1.5 \times 10^{-11} M_\odot$.year^{-1}, $t(p_{cr})$ becomes $\sim 10^7$years.

For $P > P_{cr}$, plasma can also penetrate the light cylinder since the pressure of the plasma (or material stress) ($\rho v^2 \sim r^{-5/2}$) grows quicker than the pressure of the electromagnetic field and the high energy particles ($\propto r^{-2}$) for $r_{cap} > r > r_{cyl}$. Penetration of the plasma inside the light cylinder inhibits pulsar operation and luminosity of the pulsar diminishes(since the electromagnetic field is confined inside the light cylinder).

For $r < r_{cyl}$, plasma starts to be affected by the magnetic field lines of the neutron star's dipolar magnetic field. In this case, the magnetic pressure is proportional to r^{-6} ($B^2 \sim (B/r^3)^2$), whereas the plasma pressure is still proportional to $r^{-5/2}$, that is the magnetic pressure grows faster than the plasma pressure. At the radius r_A, called the *magnetospheric radius* or *Alfven radius* where the pressure of the magnetic field is equal to the plasma pressure, plasma is stopped by the magnetic field lines and forced to corotate with the neutron star. Alfven radius can be found from the balance condition between the magnetic pressure and the plasma pressure as

$$\frac{B^2(r_A)}{8\pi} = \frac{1}{2}\rho(r_A)v^2(r_A) \tag{3.9}$$

where $\rho(r_A)$ is the density of the plasma which can be found using Equation (3.4) and $v(r_A)$ is the free fall velocity at Alfven radius which can be written as

$$v(r_A) \simeq \left(\frac{2GM}{r_A}\right)^{1/2} \tag{3.10}$$

Using Equations (3.1), (3.44), (3.9), and (3.10), we can express the Alfven radius as

$$r_A = \left(\frac{\mu^4 GM}{2L^2R^2}\right)^{1/7}$$

$$= 3.5 \times 10^8 \text{cm} \left(\frac{L}{10^{37} erg.s^{-1}}\right)^{-2/7}$$

$$\times \left(\frac{\mu}{10^{30}\text{Gauss.cm}^3}\right)^{4/7} \left(\frac{M}{M_\odot}\right)^{1/7} \left(\frac{R}{10^6\text{cm}}\right)^{-2/7}. \tag{3.11}$$

If the angular velocity of the field lines at r_A is greater than that of the Keplerian orbit at r_A, then the plasma cannot reach the neutron star's surface since centrifugal force prevents material from entering the magnetosphere. Moreover, plasma is thrown away due to the misalignment between the magnetic axis and the spin axis: The magnetic axis, in general, is misaligned with the spin axis, so the magnetic pressure on the plasma is not constant over a spin period by the plasma and in this case the magnetic field lines are like a *propeller*.If the velocity of this propeller exceeds the velocity of sound in this plasma ("supersonic propeller"), then shock-waves are generated heating the plasma and leading to its

outflow. In the subsonic propeller case, on the other hand, the magnetic field lines are not expected to cause any dissipation if the plasma is assumed to be inviscid. However, if there is a finite viscosity of the plasma then the rotating magnetic field lines are expected to generate turbulent motion in the plasma(Davies et al. 1979). So, even in subsonic case, a propeller mechanism is expected to occur[4].

Interaction of the disk and the magnetic field lines cause a spin-down until the period of the neutron star reaches

$$P = P_{accr} = 2\pi r_A^{3/2}(GM)^{-1/2}. \tag{3.12}$$

At this period, the magnetic field lines at r_A rotate at the Keplerian orbit's velocity, so for the periods greater than P_{accr} the centrifugal barrier no longer exists, and plasma can be trapped by the field lines. The deceleration time to this period can be found by using $I\omega\frac{d\omega}{dt} = -\dot{M}\frac{GM}{r_m}$ and $P = \frac{2\pi}{\omega} = \frac{P_{cr}}{(1-\frac{t}{t_{accr}})^{1/2}}$ which are valid till $P = P_{accr}$. So,

$$t_{accr} = \frac{4r_m cv}{GM} t(P_{cr}) \tag{3.13}$$

Typical value for t_{accr} is about 10^8years for the same quantities used for the $t(P_{cr})$ calculation.

The above consideration about the initial spin-down to the accretion period is valid if and only if r_A is smaller than the gravitational capture radius r_{capt}. If $r_A > r_{capt}$ is the case, then the gravitation becomes unimportant and reaching

[4] Even if the magnetic axis is aligned with the spin axis, there may still be a spin-down due to the friction between the surface of the magnetospheric boundary and the surrounding plasma(Lipunov 1992; Mineshige et al. 1991).

the period P_{accr} is not sufficient for accretion. This is similar to the interaction of the solar wind with the Earth's magnetosphere, so the neutron star is classified as a *georotator* instead of an *accretor*(Lipunov 1987). So, initial spin-down is followed by two different possibilities:

$$\text{Ejector} \rightarrow \text{Propeller} \rightarrow \text{Accretor (for } r_A < r_{capt})$$

$$\text{OR}$$

$$\text{Ejector} \rightarrow \text{Propeller} \rightarrow \text{Georotator (for } r_A > r_{capt})$$

However, due to their strong magnetic fields, georotator stage should not be common for the neutron stars.

For an accreting neutron star in a binary system, there are basically two mass transfer types from the companion star: transfer via companion's wind and transfer via Roche lobe overflow. If a neutron star accretes plasma from the companion's wind, it is expected to capture only a fraction of the total material exhausted if we assume isotropic formation and propagation of the wind, since

$$\frac{\dot{M}}{\dot{W}} = \frac{\pi r_{capt}^2}{4\pi A^2} = 2.5 \times 10^{-3} \left[\frac{r_{capt}}{10^{10} cm}\right]^2 \left[\frac{A}{10^{11} cm}\right]^{-2} \tag{3.14}$$

where A is the binary separation and $\dot{W}$ is the rate of mass loss from the companion.

Equation (3.14) shows that, accretion from a wind can only be effective for massive X-ray binaries that include massive companions having strong stellar winds. An accretion disk may form in wind-fed systems if the captured material has sufficient angular momentum to circularize before reaching the neutron

star magnetosphere. For an accretion disk to form, the mean specific angular momentum (l_{mean}) of the captured plasma is estimated to be about (King 1995)

$$l_{mean} \simeq \eta \frac{r_{capt}^2}{4} \frac{2\pi}{P_{orb}} \tag{3.15}$$

where $\eta \sim 1$ is an efficiency factor and P_{orb} is the orbital period of the binary system.

Another type of mass transfer is the mass transfer via Roche lobe overflow. If the companion star has a volume that fits its Roche lobe, then plasma on its surface flows through the inner Lagrangian point to the neutron star's vicinity. In this process, a part of the angular momentum of the orbital rotation is carried by the plasma. This angular momentum always satisfies Equation (3.15), so an accretion disk is always expected to form.

When an accretion disk forms around the neutron star, there are several different regions around the neutron star according to the disk's interaction with the plasma as (Ghosh & Lamb 1991,1979b):

1. The region between r_{capt} (capture radius) and r_s (screening radius) where the effect of the magnetic field of the neutron star is negligible,

2. The region between r_s and r_0 (the radius inside which the angular velocity of the plasma starts to decrease to the neutron star's angular velocity) where magnetic field lines begin to thread the disk without disrupting the disk completely. This region is called *outer transition zone*,

3. The region between r_0 and r_A. This region is called *inner transition zone*.

In this region magnetic field lines begin to force the plasma to rotate with the neutron star's angular velocity. The width of this region is small compared to r_A, since magnetic stress is proportional to r^{-6}, whereas material stress is just proportional to $r^{-5/2}$.

4. The region between r_A and R (radius of the neutron star) where plasma accretes to the neutron star by flowing through the magnetic field lines (no disk formation is possible).

Discussion about the accretion disks in this chapter will be based on the α-disk model unless stated otherwise. According to this model, the disk is assumed to be a geometrically thin Keplerian disk having the following properties (Ghosh & Lamb 1991):

1. Accretion flow is steady.

2. The flow is axially symmetric, so it has no dependence on the azimuthal direction.

3. The flow is symmetric with respect to the plane z=0 (the plane of the orbital rotation), so vertical structure of the disk depends on $|z|$.

4. Semi-thickness h at radius r is small compared to r (the disk is geometrically thin).

5. The azimuthal motion is closely Keplerian.

6. $|v_z| \ll |v_r| \ll |v_\phi|$, where these quantities are the magnitudes of vertical, radial and azimuthal velocities.

7. The radial pressure gradient and heat flux are negligible.

8. Contribution of the viscous stress to the total torque exerted by the disk

on the neutron star is negligible.

3.3 Torques Exerted by Accretion Disks

Torques on the disk accreting neutron stars in binaries can be exerted via the interaction of the disk with the magnetosphere of the neutron star. The region between r_s and r_0 (outer transition zone) and the region between r_0 and r_A (inner transition zone) are the only regions where the angular momentum exchange between the disk and the neutron star is realized.

Interaction between the disk and the magnetic field lines in the outer transition zone is by means of the threading of the field lines through the disk. Because of the high conductivity of the disk (since it is formed by the conducting plasma), it may be plausible to think that the neutron star's magnetic field lines cannot penetrate the disk[5], so the disk squeezes in between the field lines (Anzer & Börner 1980). However, in general partial threading of the magnetic field lines is possible with the *Kelvin-Helmholtz instability*, *turbulent diffusion*, and the *magnetic field reconnection* processes(Ghosh & Lamb 1991; Ghosh & Lamb 1979a).

The *Kelvin-Helmholtz instability* is caused by the velocity discontinuity between the low-density magnetic field region and the disk. Threading of the magnetic field lines with this instability is possible if unstable modes grow to an amplitude comparable to the semi-thickness h of the disk. For the unstable modes, the ratio of the radial-drift time of the disk ($\tau_d \sim r\,|v_r|^{-1} \sim 10^3 s$) to the

[5] Because the surface currents of the disk shield the disk material from the neutron star's dipolar magnetic field.

linear growth time of the instability τ_{KH} is about 10^5(Ghosh & Lamb 1979a). This means that there is enough time for these modes to grow to a sufficiently large amplitude to disturb the disk surface and allow the neutron star's magnetic field to mix with the disk plasma, producing a couple between the disk and the neutron star.

Turbulent diffusion is due to the convection caused by the vertical temperature gradient in the disk. The external magnetic field vertically diffuses in a time $\tau_t \sim h^2\lambda^{-1}$ where λ is the turbulent diffusivity (typically $\lambda \ll 1cm^2s^{-1}$). The ratio τ_d/τ_t is about 10^3(Ghosh & Lamb 1979a),implying the possibility for the field lines to thread the disk.

Reconnection is the process of the combination of the small-scale magnetic field within the plasma with the magnetic field of the neutron star. It is found that the ratio of the radial drift time (τ_d) to reconnection time (τ_r) is about 10^3. So, reconnection can produce a couple between the disk and the neutron star like Kelvin-Helmholtz instability and turbulent diffusion[6].

Interaction of the magnetic field lines and the plasma in the inner transition zone is due to the material stress of the plasma. In this case, plasma interacts with the corotating magnetosphere and the angular momentum of the plasma is transferred to the magnetosphere.

In general the accretion torque produced by flow of plasma onto a neutron star can be written as(Ghosh & Lamb 1991):

[6] All of the time scales discussed in the last three paragrahs are for $\mu \sim 10^{30}$Gauss.cm^3,$M \sim M_\odot$, and $\dot{M} \sim (10^{-9} - 10^{-8})M_\odot$.year^{-1}.

$$N = -\int_S \left(\vec{r} \times \vec{\Pi}\right) . \hat{n} ds \tag{3.16}$$

where S is the surface enclosing the neutron star, $\vec{\Pi}$ is the momentum flux density tensor, $\hat{n}$ is a unit vector normal to the surface which is directed outward, and $\vec{r}$ is the position vector originating from the center of the neutron star. For an axisymmetric steady accretion, this integral can be written in the form (Ghosh & Lamb 1991, 1979b):

$$N = \int_S \left(-\sigma \varpi^2 \Omega \vec{v_p} + \varpi \frac{B_\phi \vec{B_p}}{4\pi} + \eta \varpi^2 \nabla \Omega\right) . \hat{n} ds \tag{3.17}$$

where ϖ is the radius in cylindrical coordinates centered on the neutron star and aligned with the stellar rotation axis, σ is the plasma mass density, Ω and v_p are the angular and poloidal velocities of the plasma, B_p and B_ϕ are the poloidal and azimuthal components of the neutron star's magnetic field, and η is the effective dynamic viscosity. In this equation, the first, second and third terms represent material, magnetic and viscous stresses. Assuming that viscosity is negligible, the third term can be neglected.

It is convenient to evaluate Equation (3.17) from a surface S that consists of three parts (See Figure (3.1)): (1) A cylindrical surface S_1 at the radius r_0, (2)a surface S_2 consisting of two sheets above and below the disk starting from r_0 ending at infinity, and (3) Two hemispherical surfaces (S_3) at infinity.

The resultant torque N is the sum of the torques exerted from S_1, S_2, and S_3:

Figure 3.1: Side view of the accretion flow and the surfaces used to evaluate Equation (3.17) (Ghosh & Lamb 1979b)

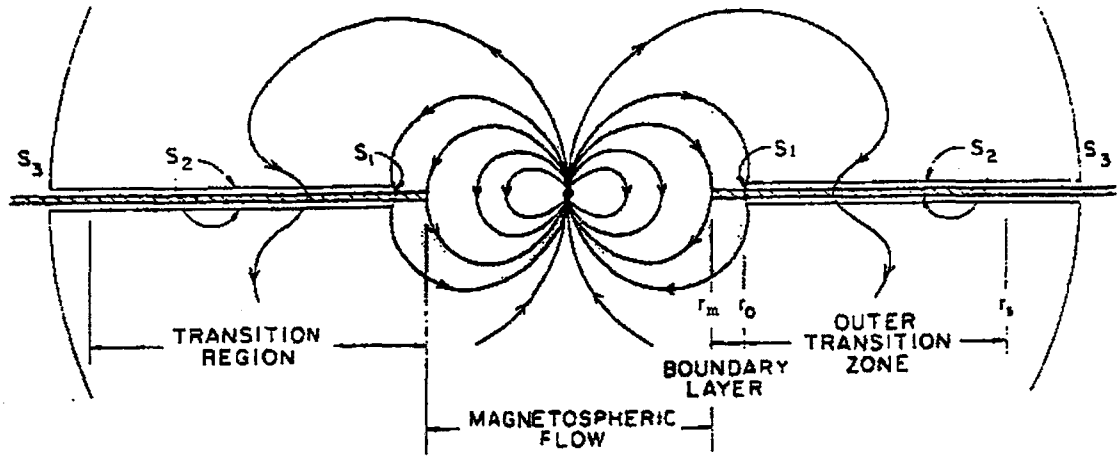

$$N = N_1 + N_2 + N_3 \tag{3.18}$$

The torque N_1 is determined by the material stress term, because the magnetic stress has no component perpendicular to S_1. So, using Equation (3.17):

$$N_1 = \sigma v_r r_0^2 \Omega_K(r_0) \times 2\pi r_0 \times 2h$$

$$= \left(\frac{\dot{M}}{4\pi r_0 h v_r}\right) \times v_r \times r_0^2 \times \left(\frac{GM}{r_0^3}\right)^{1/2} \times 2\pi r_0 \times 2h$$

$$= \dot{M} \, (GMr_0)^{1/2} \tag{3.19}$$

where $\Omega_K(r) = (GM/r^3)^{1/2}$ is the Keplerian angular velocity at radius r, and h is the semithickness of the disk.

The torque N_2 is, in contrast, determined by the magnetic stress on S_2, since no material stress on S_2 is present ($\rho \to 0$ at the surface). So[7]:

$$N_2 = \int_{S_2} (rB_z B_\phi / 4\pi) ds \tag{3.20}$$

Ghosh and Lamb (Ghosh & Lamb 1991, 1979a, 1979b) parametrize the total torque in terms of the dimensionless torque n, so that

$$N = n(\omega_s) N_1 \tag{3.21}$$

where the dimensionless torque can be found as

$$n(\omega_s) = 1 + \frac{1}{2}(1-\omega_s)^{-1} \times \int_1^{y_s} b_{out}(y) \left(y^{-3/2} - \omega_s\right) y^{-31/40} dy \tag{3.22}$$

In this equation, ω_s is called *fastness parameter*, being equal to

$$\omega_s = \frac{\Omega_s}{\Omega_K(r_0)} \tag{3.23}$$

where Ω_s is the angular velocity of the neutron star and its corotating magnetosphere. In Equation (3.22), $y = r/r_0$ is the dimensionless radius, y_s is the dimensionless screening radius, and $b_{out}(y)$ is the dimensionless poloidal magnetic field (Ghosh & Lamb 1979a).

For a slowly rotating neutron star ($\omega_s \ll 1$), n takes its maximum value becoming ≈ 1.4. This corresponds to a maximum spin-up torque. In general,

[7] The angular motion of the disk plasma with respect to the neutron star stretches the stellar field lines in the azimuthal direction, so B_ϕ is generated. Similarly, the radial flow of the plasma compresses and amplifies this azimuthal field.

n decreases with increasing ω_s, and there is a certain ω_c above which a net-spin down torque exists ($\omega_c \sim 0.35$).Above a certain $\omega_{\max}$ (≈ 0.95), no steady accretion is predicted.

The dimensionless torque can be approximately written as (Ghosh & Lamb 1991)

$$n(\omega_s) = 1.4\left(\frac{1-\omega_s/\omega_c}{1-\omega_s}\right) \tag{3.24}$$

When the torques N_1 and N_2 are separately considered, the nature of the resultant torque can be explained. For $\omega_s < 1$, the torque N_1 always gives a spin-up contribution since it carries additional angular momentum to the neutron star. On the other hand, the torque N_2 can cause either a spin-up or a spin-down torque. Azimuthal pitch of the field lines changes sign at the corotation radius r_{co} where the angular velocity of the Keplerian orbit is the same as the angular velocity of the neutron star ($r_{co} = (GM/\Omega_s^2)^{1/3}$ where $\Omega_s = \Omega_K(r_{co})$). So, part of N_2 causes spin-up for $r_0 < r < r_{co}$, and part of N_2 causes spin down for $r_{co} < r < r_s$. This implies that for slow rotators $N_2 > 0$ (since $r_0 \ll r_{co}$), for moderately fast rotators $N_2 < 0$, and for very fast rotators $-N_2 > N_1$ ($r_0 \approx r_{co}$) causing a net spin-down.

Ghosh and Lamb (Ghosh & Lamb 1979b) derive the following relation for ω_s in terms of the period, mass accretion rate, magnetic moment and the mass of the neutron star as:

$$\omega_s = 1.19 P^{-1} \left[\frac{\dot{M}}{10^{-9} M_\odot \mathrm{year}^{-1}}\right]^{-3/7} \left[\frac{\mu}{10^{30} \mathrm{Gauss.cm}^3}\right]^{6/7} \left[\frac{M}{M_\odot}\right]^{-5/7} \qquad (3.25)$$

This equation comes from the fact that the structure of the magnetosphere and the transition zone is mainly determined by the plasma accretion rate together with the magnetic field strength and the mass of the neutron star.

Equation (3.25) has two important implications. The first one is about the change of ω_s with the magnetic field. If there is a decay in the magnetic field of the neutron star, then ω_s is expected to get smaller implying that the dimensionless torque n gets greater in positive sense(spin-up). The second implication of Equation (3.25) is that a change in plasma accretion rate has an important effect on ω_s. For very large plasma accretion rate, the slow rotator condition holds, and for very small mass accretion rate, even $\omega_s = \omega_{\mathrm{max}}$ situation can be reached.

The net torque estimated in Equation (3.21), was in good agreement with the earlier observations of accretion powered pulsars Her X-1 and Cen X-3 both of which were thought to be accreting via persistent accretion disks(Elsner & Lamb, 1977; Ghosh & Lamb 1979). However, BATSE observations of some accretion powered pulsars (including Cen X-3) show that the torques are bimodal, alternating from spin-up and spin-down, and time for transition between spin-up and spin-down is shorter than BATSE can resolve($\lesssim$ 10 days)(Nelson et al. 1997, Bildsten et al. 1997). Episodes of spin-down range from $\sim$ 60days (Cen X-3, OAO 1657-415) to $\sim$ years (GX 1+4, 4U 1626-67).

According to the conventional accretion disk theory (Ghosh & Lamb 1979b),

this type of torque reversal can be due to the fact that the neutron star spins in a critical period so that overall torque oscillates around 0 (that means $\omega_s = \omega_c \sim 0.35$). However, this explanation does not explain bimodal behaviour of the spin frequency, i.e observations show that there are distinct spin-up and spin-down episodes with torques similar in magnitude but opposite in direction. This may be possible when there are stepwise changes in $\dot{M}$. But, these stepwise changes would also change the X-ray luminosity considerably since $L \propto \dot{M}$, but no significant luminosity difference could be observed.

Spin-down episodes of these accretion powered pulsars can be explained by assuming a retrograde Keplerian accretion disk (Nelson et al. 1997). This accretion disk has the same properties except that it rotates in the opposite sense with the spin direction of the neutron star (also opposite sense with the direction of the orbital angular momentum). However, it is not possible to form a retrograde accretion disk in the case of accretion via Roche lobe overflow. From simulations, it is shown that it is possible to form retrograde disks in the case of accretion via fast wind originating from an OB or Be star(*See* e.g Blondin et al. 1990, Matsuda et al. 1991) or slow wind orginating from a red giant for a particular pulsar GX 1+4 (Murray et al. 1998).

Another explanation for the torque reversals in accretion powered pulsars is made by Yi et al.(1997). According to this explanation, a critical mass accretion rate (with $\dot{M} \sim 10^{15} - 10^{16} \mathrm{g.s}^{-1}$) may lead to a radially advective sub-Keplerian accretion disk with the new angular frequency Ω' being

$$\Omega'(r) = A\Omega_K(r), \tag{3.26}$$

where $A \simeq 0.2$. According to this new rotation rate of the disk, corotation radius and fastness parameter can be rewritten as

$$r'_{co} = A^{2/3} r_{co} \tag{3.27}$$

and

$$\omega'_s = \frac{\omega_s}{A} \propto \frac{\dot{M}^{-3/7} B^{6/7}}{A}. \tag{3.28}$$

Equation (3.28) implies that a transition from spin-up to spin-down is possible in case of a transition from a Keplerian disk to a sub-Keplerian one with $A \simeq 0.2$, since this transition of the disk increases the fastness parameter considerably. However, observations show that $\dot{M}$ is $\sim 10^{17} - 10^{18}$g.s^{-1}, much larger than the critical mass accretion rate for advection, so that the disks of observed neutron star binaries should always be in the same state(Nelson et al. 1997; Nagase et al. 1989).

Recently, van Kerkwijk et al.(1998) suggest that the torque reversals observed in some of the accretion powered pulsars may be due to the disk being warped to such an extent that the inner region becomes tilted by more than 90 degrees. This means that the inner region becomes retrograde, leading to a negative torque. However, timescale of this phenomenon is unclear. Moreover, no mechanism is suggested to restore the original prograde configuration of the disk.

T.C. YÜKSEKÖĞRETİM KURULU
DOKÜMANTASYON MERKEZİ

3.4 Inner Disk Models and X-ray Luminosity and Torque Correlations as Diagnosis of Disk Accretion

In the previous section, we deal with the torques estimated by the Ghosh& Lamb model (Ghosh&Lamb 1979b,1991). This analysis can be expanded by using different inner disk models.

Let us consider a neutron star with dipole magnetic field $\sim 10^{11} - 10^{12}$ Gauss. If we have a Keplerian accretion disk around this neutron star, we expect this disk to be terminated at $\sim 10^8 - 10^9$ cm for an accretion rate $\sim 10^{17} - 10^{18}$ g.s^{-1}(Ghosh & Lamb 1978, 1979a,b). Termination radius of the disk corresponds to the middle region of a Shakura-Sunyaev accretion disk, which is optically thick and gas pressure dominated (GPD) with electron scattering free-free absorption (Shakura & Sunyaev 1973, Ghosh & Lamb 1992). This corresponds to a one temperature inner disk model abbreviated as '1T Opt thick GPD (1G)'. The inner radius of the Keplerian accretion disk around a neutron star with weak dipole magnetic field ($\sim 10^8 - 10^9$ Gauss) becomes $\sim 10^6 - 10^7$ cm. For a Shakura-Sunyaev disk, this corresponds to inner radiation pressure dominated (RPD) region of the accretion disk which is thermally and viscously unstable, so an alternative RPD model, β-model, can be considered (Ghosh & Lamb 1992). This model is also a one temperature inner disk model abbreviated as '1T Opt thick RPD (1R)'.

There is another class of inner disk models where the disk is assumed to be optically thin in the vertical direction (Ghosh & Lamb 1992). In such disks ions

are much hotter than electrons and both of these species are much hotter than the gas in optically thick disks, and disk is GPD. Two models of 2 temperature GPD inner disk models can be considered: '2T Opt thin GPD Compt brems (2B)' for which the electrons are cooled by Comptonizing soft photons coming from an external source (Shapiro et al. 1976), and '2T Opt thin GPD Compt soft photon (2S)' for which the cooling mechanism is Comptonized bremsstrahlung (White & Lightman 1989,1990).

Let us consider a neutron star accreting from the disk with inner radius r_0, which can be expressed for any inner disk model as (Ghosh & Lamb 1992)

$$r_0 \propto \dot{M}^a \mu^b M^c \tag{3.29}$$

where $\dot{M}$ is the mass accretion rate, μ is the magnetic moment and M is the mass of the neutron star. The values of a, b and c depend on the particular inner disk model being considered (See Table (3.1)). In the classical approach, a,b and c are $-\frac{2}{7}$, $\frac{4}{7}$, and $-\frac{1}{7}$ (Ghosh & Lamb 1979b).

If the neutron star is being spun-up by accretion and the spin-up torque is mainly due to the angular momentum carried by the material accreting from the disk, then the torque on the neutron star and the X-ray luminosity can be written as

$$\tau = I\dot{\Omega} \approx \dot{M}\,(GMr_0)^{1/2}\,, \tag{3.30}$$

$$L_x \approx \frac{GM\dot{M}}{R_x}, \tag{3.31}$$

Disk Model	Value of a	Value of b	Value of c
1T Opt Thick GPD (1G)	-0.25	0.58	-0.21
1T Opt Thick RPD (1R)	-0.15	0.51	-0.13
2T Opt Thin GPD Compt brems (2B)	-0.48	0.57	0.05
2T Opt Thin GPD Compt soft photon (2S)	-1.70	0.80	0.73

Table 3.1: Scaling of r_0 where $r_0 \propto \dot{M}^a \mu^b M^c$ (Ghosh & Lamb 1992).

where I is the moment of inertia, $\dot{\Omega}$ is the angular frequency derivative ($\dot{\Omega} = 2\pi\dot{\nu}$), and R_x is the radius of the neutron star. We can rewrite $\dot{\Omega}$ as

$$\dot{\Omega} \approx \frac{G^{\frac{1}{2}} M^{\frac{1}{2}(c+1)} \dot{M}^{1+\frac{1}{2}a} \mu^{\frac{b}{2}}}{I}. \tag{3.32}$$

Thus, we can relate $\dot{\Omega}$ to L;

$$\dot{\Omega} = \left[\xi^{\frac{1}{2}} \frac{G^{-\frac{1}{2}(2\alpha-1)} M^{\frac{1}{2}(c-2\alpha+1)} \mu^{\frac{b}{2}} R_x^{\alpha}}{I} \right] L^{\alpha} \tag{3.33}$$

where $\alpha = 1 + \frac{1}{2}a$ and $\xi = \frac{r_0}{\dot{M}^a \mu^b M^c} \sim 1$. After determining α and obtaining bolometric X-ray luminosity, we can choose a suitable disk model and calculate the surface dipole magnetic field using the following expression that can be derived from Equation (3.33):

$$\mu \simeq \left[\frac{\dot{\Omega} I}{(R_x L)^{\alpha}} G^{-\frac{1}{2}(2\alpha-1)} M^{\frac{1}{2}(c-2\alpha+1)} \right]^{-\frac{b}{2}} \tag{3.34}$$

In conclusion, if we can find a relation of the form $\dot{\Omega} \propto L^{\alpha}$ from observations, we can say that the X-ray pulsar is accreting from an accretion disk. If we further find α precisely, we can even conclude the type of the inner disk.

3.5 Torques in the Absence of the Keplerian Disk

If the neutron star accretes from a wind, then the radial velocity of the plasma near the capture radius is expected to be large implying a large plasma pressure, so the neutron star's magnetic field is confined to the interior of a magnetospheric cavity whose radius is much smaller than r_{capt} (Ghosh & Lamb 1979b). So, the material stress dominates and the torque becomes

$$N = \dot{J}_s = \frac{d}{dt}(I\Omega_s) = \dot{M}\, l \tag{3.35}$$

where l is the specific angular momentum of the accreting plasma at r_{capt}, $J_s(=I\Omega_s)$ is the angular momentum of the neutron star[8].

There are basically three sources for a non-zero specific angular momentum of the captured plasma (Illarionov & Sunyaev 1975):

1. **Orbital motion of the neutron star:** Considering the flow of the captured plasma in the cylinder with radius r_{capt} and then considering a thin cylindrical cross-section, one can see that the velocities of different particles in this cylinder differ due to the orbital motion by an amount $\Delta V = \Omega s$, where s is the particle impact parameter and Ω is the orbital angular velocity. So, the specific angular momentum is approximately equal to the specific angular momentum of the homogenous disk rotating around its diameter with the angular velocity Ω :

[8] This equation can also be obtained from Equation (3.8), if the surface S is a spherical surface having radius of r_{capt}, and the torque is the result of the material stress.Equation 8 yields $l = r_{capt}^2 \Omega_{pl}$ where Ω_{pl} is the angular velocity of the plasma which is smaller than the Keplerian angular velocity Ω_K in this case.

$$l_{orbit} \approx \frac{1}{4}\Omega r_{capt}^2 \tag{3.36}$$

Note that this value is only a small fraction of the specific angular momentum of the binary system (ΩA^2).

2. **Rotation of the companion star:** This does not make a significant contribution since the radius of the companion R_0 is much smaller than the binary separation A. From the conservation of angular momentum and using the fact that the rotational velocity at the companion's surface is less than the parabolic velocity ($\Omega_0 R_0 < (2GM/R_0)^{1/2}$), the angular velocity of the wind at the distance A can be written as

$$\Omega_w = \Omega_0 \left(\frac{R_0}{A}\right)^2 < \left(\frac{2GM}{R_0^3}\right)^{1/2} \left(\frac{R_0}{A}\right)^2$$

$$\simeq \Omega \left(\frac{R_0}{A}\right)^{1/2} \ll \Omega \tag{3.37}$$

So,

$$l_{companion} \simeq \Omega_w r_{capt}^2 \ll l_{orbit} \tag{3.38}$$

3. **Spatial inhomogeneities in the wind flow:** Inhomogeneities in the wind flow may cause fluctuations in the velocity and density of the wind which may lead to fluctuations in the specific angular momentum value.

When the inhomogeneities in the wind flow are not considered, the first and the second sources cause a net specific angular momentum l which have the

same direction with the angular momentum of the neutron star if the angular momentum of the orbital revolution of the binary, rotation of the companion star, and rotation of the neutron star have the same direction.

The rate of change of angular velocity Ω_s can be written as(Ghosh & Lamb 1991):

$$\dot{\Omega}_s = (\zeta - 1)\left(\frac{d\ln I}{d\ln M}\right)\left(\frac{\dot{M}}{M}\right)\Omega_s \tag{3.39}$$

where

$$\zeta = \frac{l}{R_g^2\Omega_s}\left(\frac{d\ln M}{d\ln I}\right) = \frac{l}{\Omega_s}\frac{dM}{dI} \tag{3.40}$$

is a dimensionless parameter and

$$R_g = \sqrt{\frac{I}{M}} \tag{3.41}$$

is the *radius of gyration.* The rate of change of the rotational energy E_{rot} of the neutron star is

$$\dot{E}_{rot} = \frac{1}{2}\frac{d}{dt}\left(I\Omega_s^2\right) = 2\left(\zeta - \frac{1}{2}\right)\left(\frac{d\ln I}{d\ln M}\right)\left(\frac{\dot{M}}{M}\right)E_{rot} \tag{3.42}$$

From Equations (3.33) and (3.36), one can conclude that for $\zeta < 1/2$, the neutron star spins down while losing rotational energy, for $1/2 < \zeta < 1$, it spins down while gaining rotational energy, and for $\zeta > 1$ it spins up while gaining rotational energy.

Equation (3.30) and (3.31) take

$$l \sim \Omega r_{capt}^2 \tag{3.43}$$

Considering $R_g = \sqrt{I/M} \approx R$, and $(d \ln I/dM) \sim 1$, Equation (31) reads

$$\zeta \approx \frac{\Omega r_{capt}^2}{R\Omega_s} \tag{3.44}$$

Since $r_{capt} \gg R$, one can have $\zeta \gg 1$ even if $\Omega < \Omega_s$. So, only the spin up process takes place for the neutron star accreting from the stellar wind having high radial velocities when the inhomogeneities in the wind are not considered[9].

3.6 Numerical Studies and Observational Diagnosis of Wind Accretion

As we have discussed throughout this chapter, we primarily have two kinds of mass transfer types from the companion star to the neutron star: transfer via Roche-lobe overflow of the companion for which a prograde Keplerian accretion disk forms and transfer via stellar wind of the companion. For the latter case, observations show that the simple model consisting of accretion from a spherically symmetric wind is not a complete description of high mass X-ray binaries with wind accretion (Blondin et al. 1990 and references therein).

From the hydrodynamic simulations, it is seen that stellar wind is disrupted in the vicinity of a compact X-ray source (a neutron star for our case) which causes plasma to lose its homogeneity. The interaction of the incident flow with the shock fronts in the vicinity of the neutron star can produce temporary accretion

[9] Note that this true only for $P \geq P_{accr}$ (See Equation (3.8)).

disks (Taam& Fryxell 1988a, 1988b, 1989; Blondin et al. 1990). Formation of prograde disk is the only possibility if there is large assymetries in the wind (i.e with density inhomogeneities of scale length comparable to or smaller than the accretion radius). For the case of smaller assymetries, interaction of the plasma with the shock fronts can produce disks which circulate in prograde and retrograde directions.

Using the results of the numerical studies following points can be used to understand the accretion process around the neutron star accreting from its companion's stellar wind:

1. We expect no correlation between the torque exerted on the neutron star and X-ray flux. For an accretion from a stable accretion disk, Equation (3.33) shows that X-ray flux should be correlated with the torque. Accretion from wind does not lead to the formation of a stable disk, so we do not expect to find such a correlation for an accretion powered pulsar accreting from its companion's stellar wind.

2.We expect to find a correlation between specific angular momentum and torque for negative, near zero and positive torque values. Correlation of specific angular momentum and torque for negative and positive torques shows that there is accretion disk formation in both prograde and retrograde directions without a considerable change in mass accretion which can be seen from Equation (3.19) where $l_K = \pm(GMr_0)^{1/2}$ is the specific angular momentum obtained from the inner boundary of the disk. For the near zero values of the torque, our specific angular momentum is also near zero which shows us that the accretion flow is

radial.

3. When a temporary accretion disk forms around the neutron star, we expect an increase in specific angular momentum and decrease in mass accretion rate. This is because of the fact that plasma accumulates in the disk and rotates around the neutron star with near Keplerian velocities causing a lag in the fall of the plasma onto the neutron star's surface.. Thus, if we can find time intervals with high specific angular momentum and low mass accretion rate, we can say that accretion disk formation is probable for these intervals.

4. When the disk alternates its sense of rotation, we expect an increase in mass accretion rate. For this case, rotating disk is disrupted and plasma begins to fall radially on to the neutron star's surface causing an increase in mass accretion rate.

CHAPTER 4

BATSE OBSERVATIONS ON TRANSIENT SOURCES

In this chapter, data of 5 transient sources (2S 1417-62, GS 0834-430, GRO J1008-57, GRO J1948+32 and A 1118-616) are presented. Two of these sources (2S 1417-62 and GS 0834-430) show correlation between their frequency derivative and X-ray flux which may be the implication of a prograde accretion disk formation. For the rest of the sources, no orbital correction is present. For these sources, only frequency and flux data are presented.

4.1 X-ray Luminosity and Torque Correlated Transients 2S 1417-62 and GS 0834-430

In this section, analysis of BATSE data for 2 transient sources, 2S 1417-62 and GS 0834-430, are presented. These two sources are found to be frequency derivative and X-ray flux correlated showing a correlation between torque and X-ray lumonosity. Thus, these sources may be accreting from accretion disks (*see* Sections (3.3) and (3.4)). From Equation (3.33), we have the relation of the form $\dot{\Omega} \propto L^{\alpha}$ where α is a different constant for each inner disk model (*see* Section (3.4) and Ghosh&Lamb 1992). From BATSE observations, we can determine α from a power law fitting of the frequency derivative versus flux graphs. Our

assumption is that the trend of the bolometric X-ray luminosity is similar to that of the luminosity from 20-50keV.

4.1.1 2S 1417-62

4.1.1.1 Properties

17.6s pulsations from 2S 1417-624 was discovered by SAS-3 in 1978 (Apparao et al. 1980, Kelley et al. 1981). Its optical companion was found to be a $\sim$ 16.9th magnitude Be star (Grindlay et al. 1984). From the BATSE observations, its binary orbital period was measured to be 42.12 days from the assumption of a correlation between the flux and the accretion torque (Bildsten et al. 1997).

4.1.1.2 Results

Frequency and X-ray flux data from 2S 1417-624 cover the interval between 9600 and 9740 (J.D-2440000) (*See* Figure (3.1)). Data were reduced by making bins each covering 4 days.This source shows a spin-up trend on the whole interval. Average period at this interval is 17.6s and average period derivative is -6.41×10^{-4} s.day^{-1} (average frequency derivative is 2.07×10^{-6}Hz.day^{-1}). The flux first increases between $\sim$ 9600 (J.D-2440000) and $\sim$ 9620 (J.D-2440000). Then, no significant change in flux is seen between $\sim$ 9620 (J.D-2440000) and $\sim$ 9650 (J.D-2440000). Finally, a decrease trend in flux is seen for the rest of the interval. There is a positive correlation between the flux (F) and the time derivative of the frequency ($\dot{\Omega}$) (See Figure (3.2) and also Figure 6 in Finger et al. 1996).

Making a power law fit to find α in the relation $\dot{\Omega} \propto L^{\alpha}$, we obtain 1.48 ± 0.34

Figure 4.1: Flux and frequency of 2S 1417-62 from the BATSE CONT data. Original data were reduced by making bins each covering 4 days.

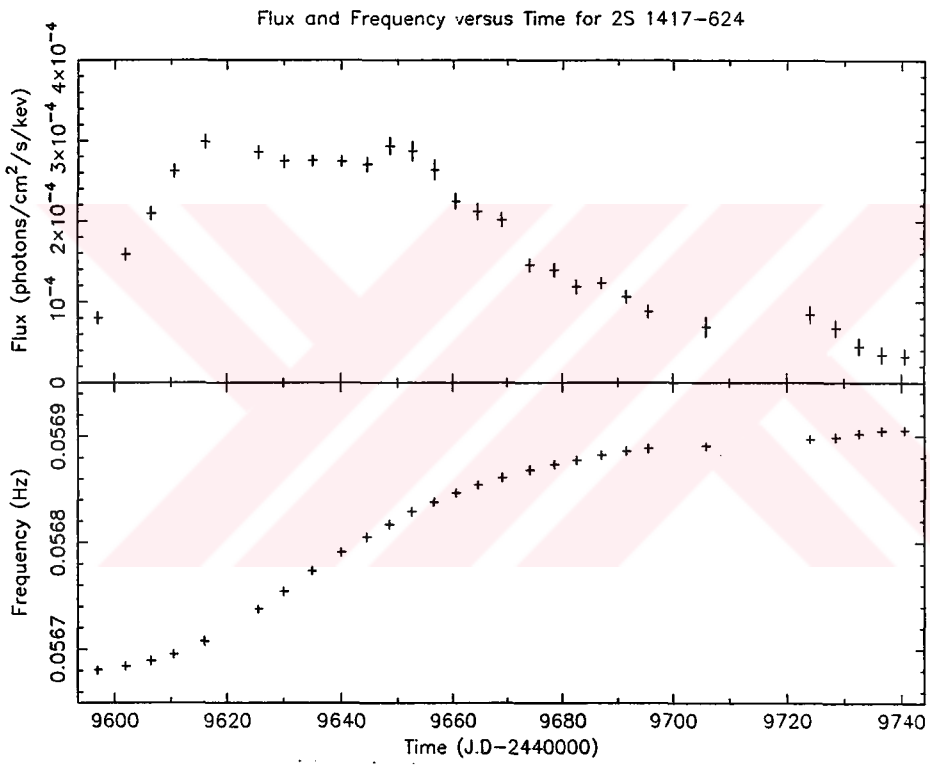

Figure 4.2: Flux versus Frequency Derivative for 2S 1417-62. Derivative of the frequency data and flux data were reduced by making bins each covering 4 days from BATSE CONT observations.

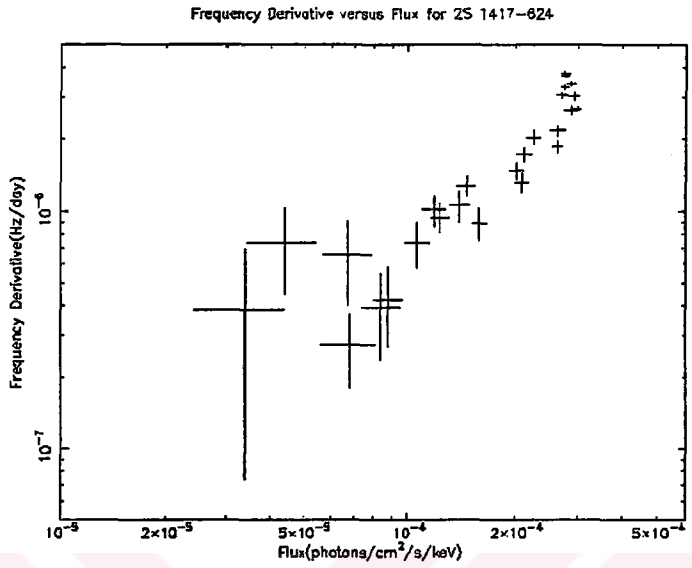

for α. For this value of α, within 2σ limits using Table (3.1), 1T Opt Thick GPD (1G), 1T Opt Thick RPD (1R) and Ghosh-Lamb models are the possible disk models for 2S 1417-624.

Knowing α, we can calculate the magnetic field using Equation (3.34) if we know the bolometric X-ray luminosity. It is given that the luminosity between 20-50keV is $\sim 1.8 \times 10^{35}$ ergs.s^{-1} (Finger et al. 1996). Assuming that luminosity between 0.5-50 keV band is approximately equal to the bolometric X-ray luminosity and using a spectral model of the form $F(E) = AE^{\lambda} \exp\left(-(E - E_{cutoff})/kT\right)$ where the best fit parameters are $F(40\text{keV}) = (5.2 \pm 0.2) \times 10^{-4}$photons.cm^{-2}s^{-1}keV^{-1}, $\lambda = 1.6 \pm 0.8$, $kT = 11.9 \pm 2.3$keV (as suggested in Finger et al. 1996), we can find the ratio of the fluxes from 0.5-50keV and 20-50keV. Multiplication of this

Figure 4.3: Cyclotron Energy versus Cut-off Energy for 9 X-ray binaries. See Table 1.6 in White et al. 1993

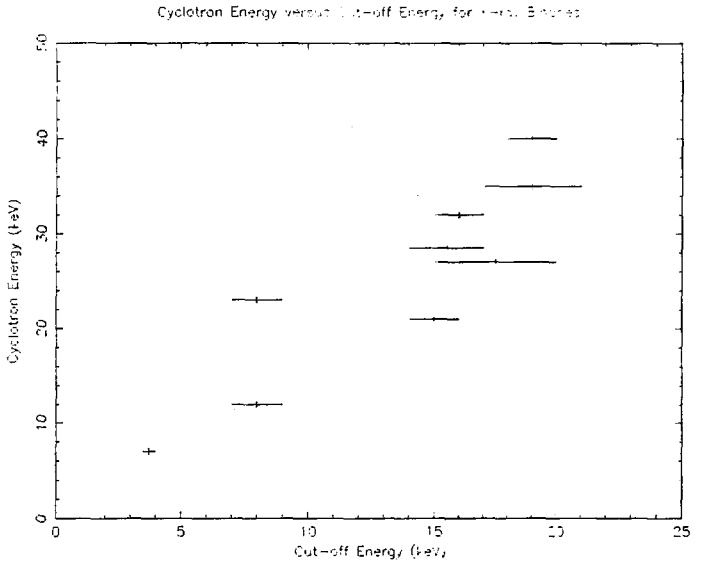

ratio by the luminosity from 20-50 keV band gives the bolometric X-ray luminosity. We perform this calculation for cut-off energies ranging from 4-20keV and we assume that cyclotron energy (E_{cyc}) is $\sim$ 1.8 times cut-off energy (E_{cutoff}) (This is obtained from the slope of the best line of the graph in Figure (4.3) which is a plot of E_{cyc} versus E_{cutoff} for 9 X-ray binaries (See Table 1.6 in White et al. 1993)). With the relation $E_{cyc} = \hbar\frac{eB}{mc}$, each cut-off energy corresponds to a magnetic field. Using this magnetic field and Equation (3.33) for a neutron star with moment of inertia 10^{45}g.cm^2, mass $1.5M_{\odot}$, radius 10^6cm, we can evaluate frequency derivative. We should note that varying photon index gives different values of bolometric X-ray luminosities, so frequency derivative also depends on the photon index we choose. From the photon index versus magnetic field graph,

we can then find the frequency derivative contours (See Figure (4.4)). Our observational frequency derivative ($\sim 10^{-11}$Hz.s^{-1}) requires a photon index $\sim 4 > 1.6$ which is higher than the model's value, so the model cannot explain the high frequency changes. Insufficiency of the model can also be verified by the luminosities it predicts: It is seen that maximum luminosities that the model gives is about 10^{37} erg.s^{-1} for photon index between 0.8-2.4. Even this luminosity is insufficient to be compatible with the frequency derivative we observed. If we use Ghosh-Lamb model and Equation (3.33), a magnetic field of $\sim 10^{12}$ Gauss is obtained if X-ray luminosity is $\sim 10^{38}$ erg.s^{-1}. So, the model is incompatible with the observations. An additional soft X-ray component to the spectral model may be required.

4.1.2 GS 0834-430

4.1.2.1 Properties

12.3s pulsations from GS 0834-430 was found by the help of subsequent observations with Ginga (Aoki et al.1992). Optical counterpart of GS 0834-430 is still unknown, but the recurrent outburst behavior indicates that it is a Be star (Bildsten et al. 1997).

4.1.2.2 Results

Frequency and X-ray flux data from GS 0834-430 cover the interval between 8375 (J.D-2440000) and 9150 (J.D-2440000).Data were reduced by making bins each covering 10 days. On this interval, there are 7 outbursts (See Figure (4.5)).

Figure 4.4: Frequency derivative contours in photon index versus logarithm of magnetic field graph for spectral model given in Finger et al. 1996. Note that Ghosh-Lamb model is used to evaluate frequency derivative values. This figure shows the impossibility for 2S 1417-624 to have a spin-up rate of $\sim 10^{-11}$Hz/s unless the photon index is ~ 4

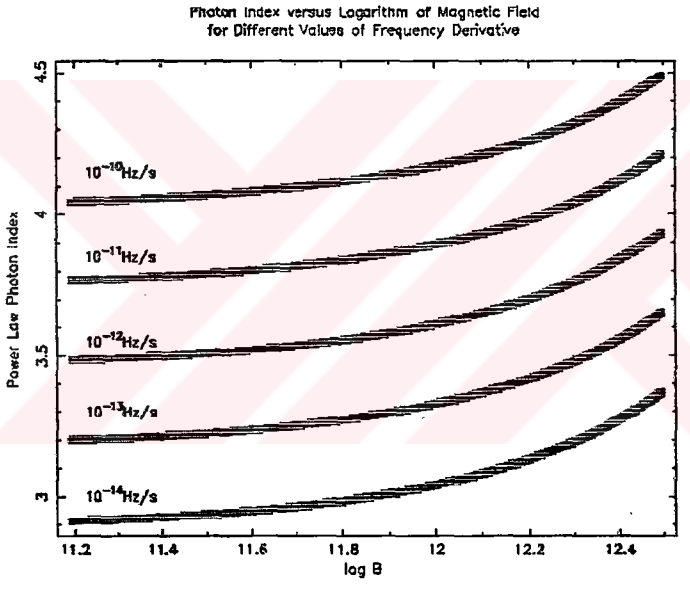

Figure 4.5: Flux and Frequency of GS 0834-430 from the BATSE CONT data. Original data were reduced by making bins each covering 10 days.

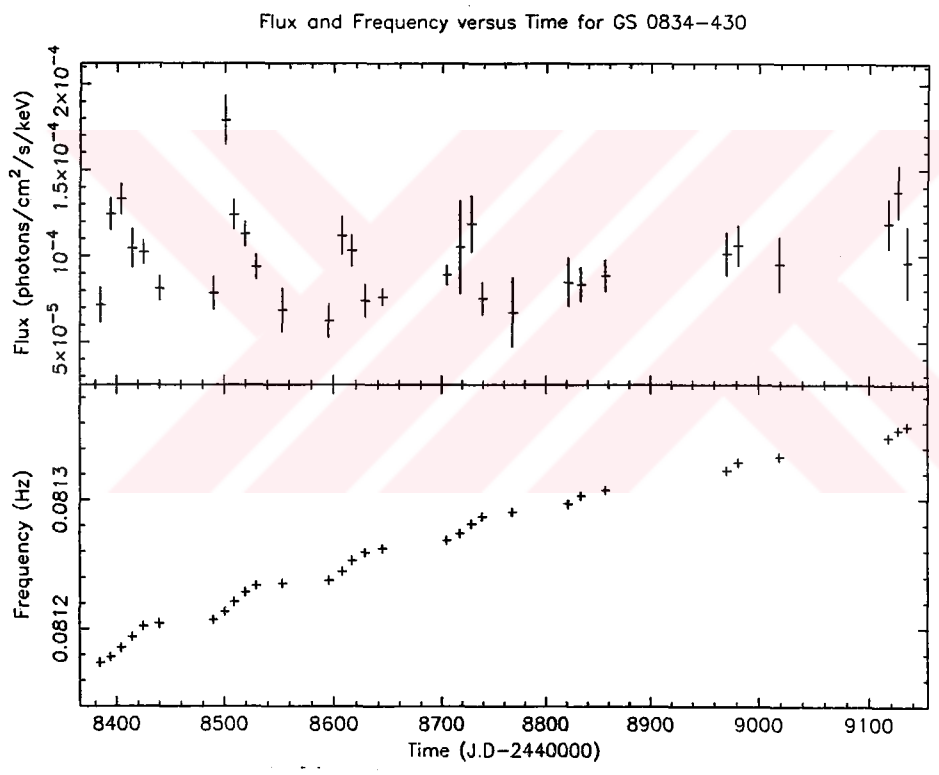

Figure 4.6: Flux versus Frequency Derivative for GS 0834-430. Derivative of the frequency data and flux data were reduced by making bins each covering 10 days.

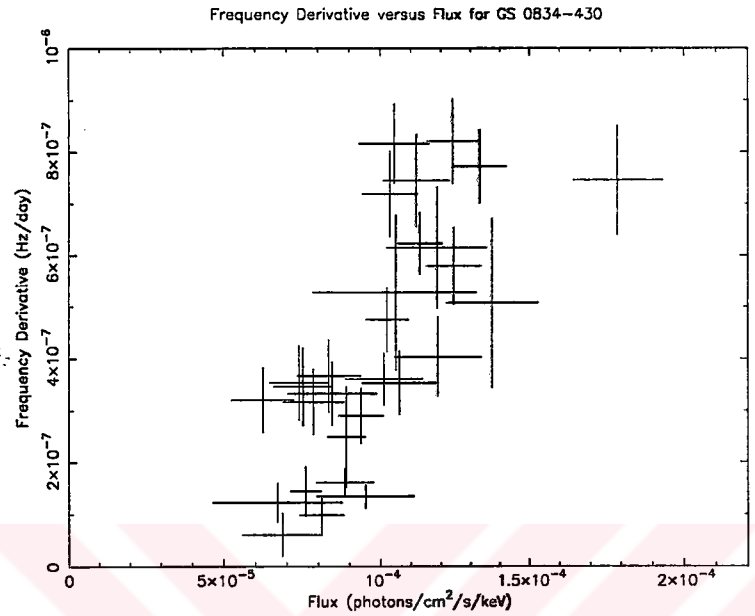

Average period on this interval is 12.3s. Average period derivative is 4.10×10^{-5}s.day^{-1}(average frequency derivative is 2.71×10^{-7}Hz.day^{-1}). There is a positive correlation between the flux and the time derivative of the frequency (See Figure (4.6)).

Making a power law fit to find α in the relation $\dot{\Omega} \propto L^{\alpha}$, we obtain 1.67 ± 0.49 for α. For this value of α, within 2σ and using Table (3.1), Ghosh-Lamb model ,1T Opt Thick GPD (1G), 1T Opt Thick RPD (1R), and 2T Opt Thin GPD Compt brems (2B) models models are the possible models.

From the power law with cut-off energy model and the count rates for GINGA LAC given (Aoki et al. 1992), flux from 1.2-27.5keV is found to be $(4.4 \mp 0.9) \times 10^{-9}$ergs.s^{-1}.cm^{-2} when an error of 20% in count rate is assumed. This flux

corresponds to an X-ray luminosity of $(1.2 \mp 0.2) \times 10^{37}$ergs.s^{-1} when distance is taken as 5 kpc. Assuming that this luminosity is approximately equal to the bolometric X-ray luminosity, the surface magnetic fields of $\sim 10^{13}$, $\sim 10^{10}$, $\sim 10^{6}$, and $\sim 10^{11}$ Gauss for 1T Opt Thick GPD ,1T Opt Thick RPD (1R), 2T Opt Thin GPD Compt brems, and Ghosh-Lamb models are found respectively using Equation(3.34) and Table (3.1) for a neutron star with moment of inertia 10^{45}gcm^2, mass $1.5M_{\odot}$, radius 10^6cm.

4.1.3 Remarks

For both of the transients 2S 1417-62 and GS 0834-430, we found a correlation between torque and X-ray luminosity. However, errors are too big for the data to have preference on a single inner disk model. If we had more data or smaller errors for each data point, we would be able to determine an inner disk model for each source.

4.2 Other Transients

4.2.1 GRO J1008-57

GRO J1008-57 is a transient pulsar which was discovered by BATSE in 1993 (Stollberg et al. 1993). Its optical companion was identified to be a Be star (Coe et al. 1994b). Its orbital period was supposed to be $\sim$ 248days which was found from the occurence of later outbursts (Bildsten et al. 1997). BATSE frequency data for this source is not orbitally corrected because of the fact that the orbital

Figure 4.7: Flux and Frequency of GRO J1008-57 from the BATSE CONT data. Original data were reduced by making bins each covering 3 days.

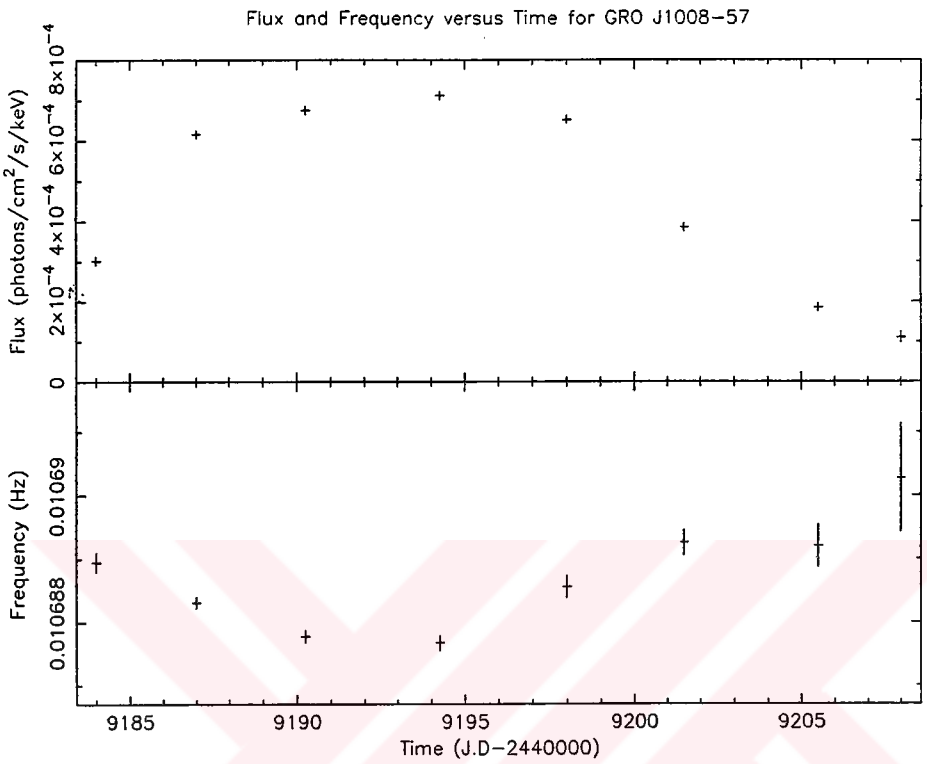

parameters are unknown. So, we cannot conclude on torque and flux.

Frequency and X-ray flux data from GRO J1008-57 cover the interval between 9183 (J.D-2440000) and 9208 (J.D-2440000) (*See* Figure (4.7)). Data were reduced by making bins each covering 3 days. This source shows a spin-down trend between $\sim$ 9183 (J.D-2440000) and $\sim$ 9193 (J.D-2440000), then a spin-up trend between $\sim$ 9193 (J.D-2440000) and $\sim$ 9208 (J.D-2440000). Average frequency on this interval is 1.07×10^{-2}Hz. There is an increase in flux between $\sim$ 9183

T.C. DOKÜMANTASYON

(J.D-2440000) and $\sim$ 9196 (J.D-2440000) and a decrease between $\sim$ 9196 (J.D-2440000) and $\sim$ 9208 (J.D-2440000). Average flux on this interval is 5.38×10^{-4} photons.cm^{-2}s^{-1}keV^{-1}.

4.2.2 GRO J1948+32

18.7s transient X-ray pulsar GRO J1948+32 was discovered by BATSE (Bildsten et al. 1997). Its companion has not been identified. BATSE frequency data for this source is not orbitally corrected since the orbital parameters are not known. So, we cannot conclude on torque and flux for this source.

Frequency and X-ray flux data from GRO J1948+32 cover the interval between 9448 (J.D-2440000) and 9483 (J.D-2440000) (*See* Figure (4.9)). Data were reduced by making bins each covering 4 days. There is a spin-down trend for about the first half and then a spin-up trend for the second half of the interval. Average frequency on the whole interval is 5.35×10^{-2}Hz. When the changes in the flux of the source is concerned, it is seen that the flux increases on the first half of the interval and then decreases on the second half. Average flux on the whole interval is 1.22×10^{-4}photons.cm^{-2}s^{-1}keV^{-1}.

4.2.3 A 1118-616

The hard X-ray transient A 1118-616 was discovered in December 1974 by the Ariel-5 satellite (Eyles et al. 1975, Ives et al. 1975). Observations have shown pulsations with a period of 405.3 ± 0.6s. Initially, these pulsations were wrongly attributed to an orbital period implying that A 1118-616 consisted of

Figure 4.8: Flux and frequency of GRO J1948+32 from the BATSE CONT data. Original data were reduced by making bins each covering 4 days.

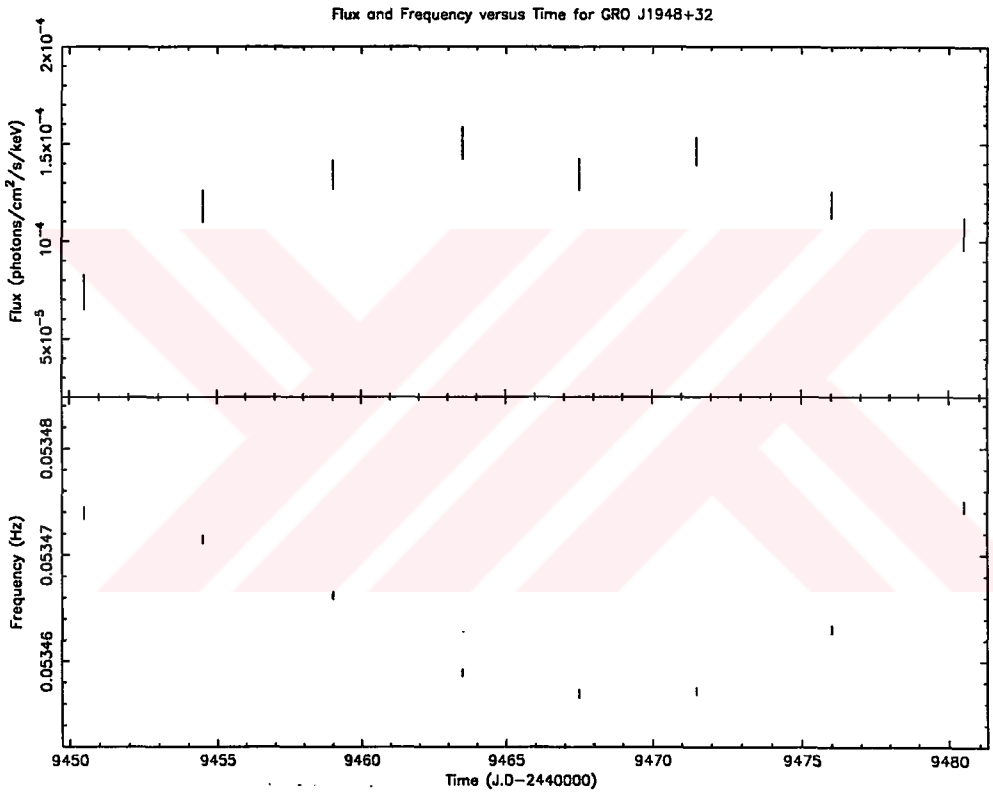

two compact objects (Ives et al. 1975). Later, it was understood that A 1118-616 consists of a compact object with the Be star companion He 3-640/Wray 793 (Heinze 1976). Since 1974, no outbursts were observed until December 1991 when BATSE detected two outbursts between 8619.5 and 8666.5 ($J.D-2440000$) (Bildsten et al. 1997).These outbursts were also observed in optical, IR and UV regions showing an increase in H_α emission and an IR excess which indicate an extended disk around the companion star(Coe et al. 1994a). BATSE frequency data for this source is not orbitally corrected since the orbital parameters are unknown. So, we cannot conclude on torque and flux for this source.

Frequency and X-ray flux data from A 1118-616 cover the interval between 8619 (J.D-2440000) and 8667 (J.D-2440000) (*See* Figure (4.11)). There exist two flares at $\sim$ 8628 (J.D-2440000) and $\sim$ 8652 (J.D-2440000) with the flux having values $\sim 8 \times 10^{-4}$ and $\sim 6 \times 10^{-4}$ photons.cm^{-2}s^{-1}keV^{-1}. Average flux on this interval is 3.9×10^{-4} photons.cm^{-2}s^{-1}keV^{-1}. Meanwhile, frequency of the source is about constant having the value 2.46×10^{-3}Hz.

Figure 4.9: Flux and frequency of A1118-616 from BATSE CONT data.

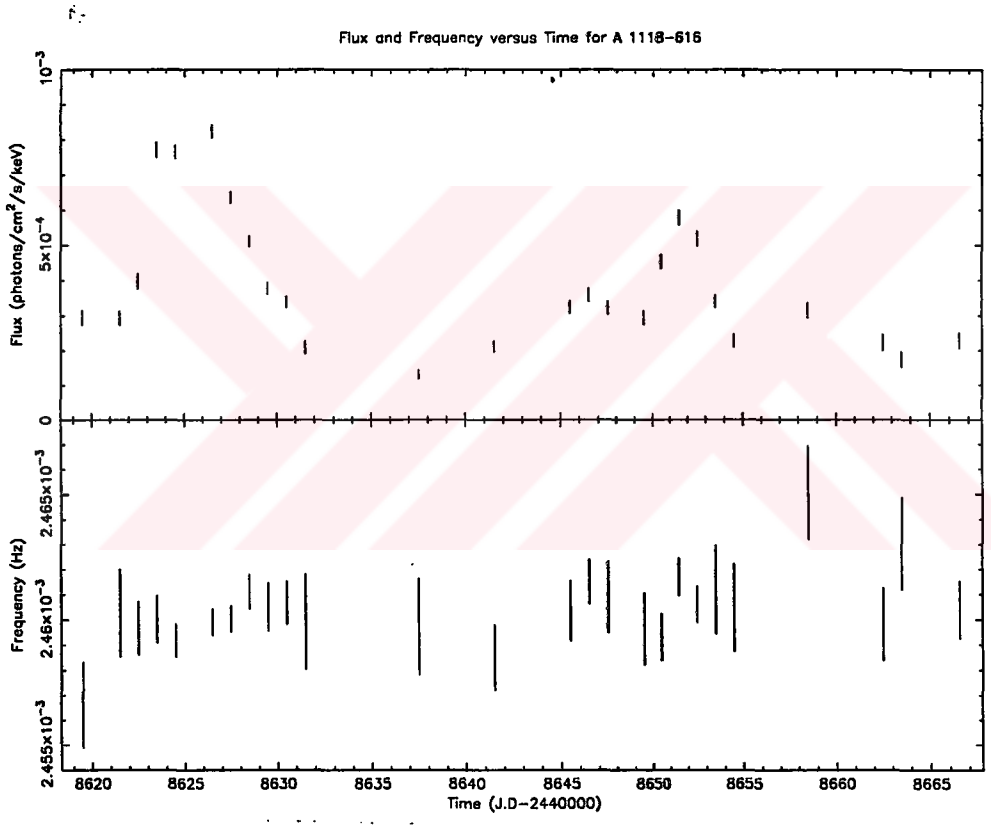

CHAPTER 5

BATSE OBSERVATIONS ON HIGH MASS SYSTEMS

In this section, analysis of BATSE data for 3 high mass systems Vela X-1, GX 301-2 and OAO 1657-415 is presented. Correlations between frequency derivative (i.e angular acceleration), flux and specific angular momentum are discussed. Similar analysis was made for OAO 1657-415 (Baykal, 1997).

The torque on the neutron star can be expressed in terms of the specific angular momentum (l) added to the neutron star by the accreted plasma and the mass accretion rate ($\dot{M}$):

$$I\dot{\Omega} = \dot{M}l \tag{5.1}$$

This equation is a general expression which is valid for both an accretion from a Keplerian disk and accretion from the stellar wind. In the case of accretion from a prograde Keplerian disk Equation (3.21) is valid. In that case we have an extra factor, a dimensionless torque $n(\omega(s))$ approximately defined in Equation (3.24), multiplied by the material torque to give the net torque exerted on the neutron star. For this case specific angular momentum is $(GMr_0)^{1/2}$. Dimensionless torque may be positive or negative depending on the fastness parameter ω_s defined in Equations (3.23) and (3.25). For a slowly rotating neutron star ($\omega_s < \omega_c$), we

expect a spin-up torque and for a very fast rotating neutron star ($\omega_s >> \omega_c$), we expect a spin-down torque. We also expect to see positive correlation between torque and mass accretion rate if the disk is prograde. For a disk formed from Roche Lobe overflow of the companion we expect the plasma to carry positive specific angular momentum, so a prograde disk should be formed and torque should be correlated with mass accretion rate.

For the case of an accretion from the wind, numerical simulations show that both prograde and retrograde Keplerian disk formation is possible (Taam& Fryxell 1988a,1988b,1989, Blondin et al. 1991, Murray et al. 1998). So, we can observe transitions from spin-up to spin-down or vice versa even if there is not a significant change in mass accretion rate[1].

In the following subsections, we try to determine whether there exist temporary prograde and retrograde disk formation for Vela X-1, GX 301-2 and OAO 1657-415 all of which are thought to be accreting from their stellar companions' wind.

5.1 Vela X-1

5.1.1 Properties

283s pulsations from Vela X-1 were discovered by *SAS-3* in 1975 (McClintock et al. 1976). It is the brightest persistent accretion powered pulsar in the 20-50

[1] It should be noted that variation in torque exerted on the neutron star can be written as $\delta\tau = I\delta\dot{\Omega} = \delta\dot{M}l + \dot{M}\delta l$. For the case of wind accretion, simulations show that there are significant changes in the specific angular momentum of the accreted matter, i.e accretion geometry changes continuosly. This makes the second term in this equation more significant

Figure 5.1: Flux and Frequency of Vela X-1 from the BATSE CONT data. Original data were reduced by making bins each covering 45 days.

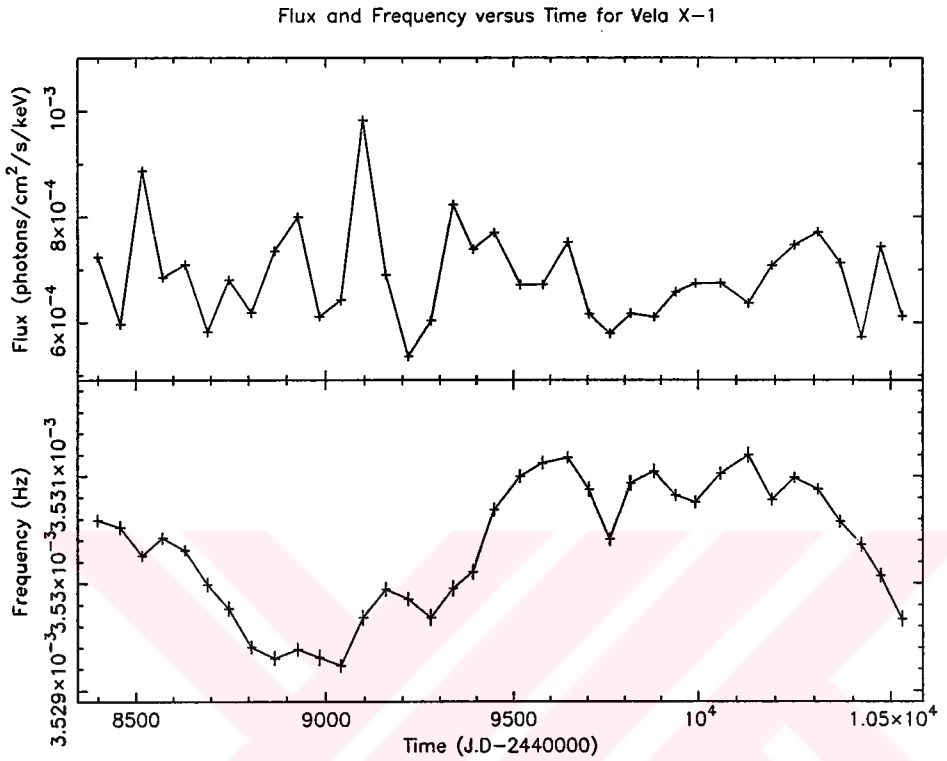

keV energy band (Bildsten et al. 1997). Optical companion of Vela X-1 is the B0.5 Ib supergiant HD77581 (Vidal et al. 1973). This system is an eclipsing binary with an eccentric orbit with 8.96days period (Rappaport et al. 1976).

5.1.2 Results

Frequency and X-ray flux data from Vela X-1 cover the interval between 8371 (J.D-2440000) and 10580 (J.D-2440000) (*See* Figure (5.1)). Data were reduced by

Figure 5.2: Frequency Derivative versus Time for Vela X-1. Original data were reduced by making bins each covering 45 days.

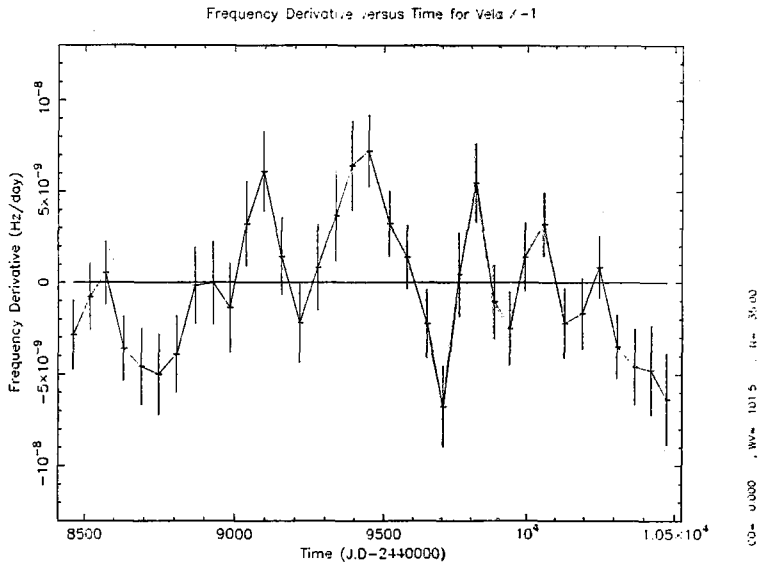

making bins each covering 45 days. Average frequency of the source on the interval is 3.53×10^{-3}Hz and average flux is average flux is 6.87×10^{-4}photons.cm^{-2}s^{-1}keV^{-1}

There is no correlation between frequency derivative and flux (*see* Figure (5.4)). This shows that there is no stable accretion disk formation for Vela X-1. From Figure (5.6), we see that there is a correlation between frequency derivative over flux and frequency derivative. Since frequency derivative over flux is directly proportional to the specific angular momentum carried by the accreted plasma, this correlation is equivalent to the correlation between frequency derivative and specific angular momentum. A correlation between frequency derivative and specific angular momentum for positive, negative and near zero values of frequency

Figure 5.3: Frequency derivative over flux versus time for Vela X-1. Original data were reduced by making bins each covering 45 days.

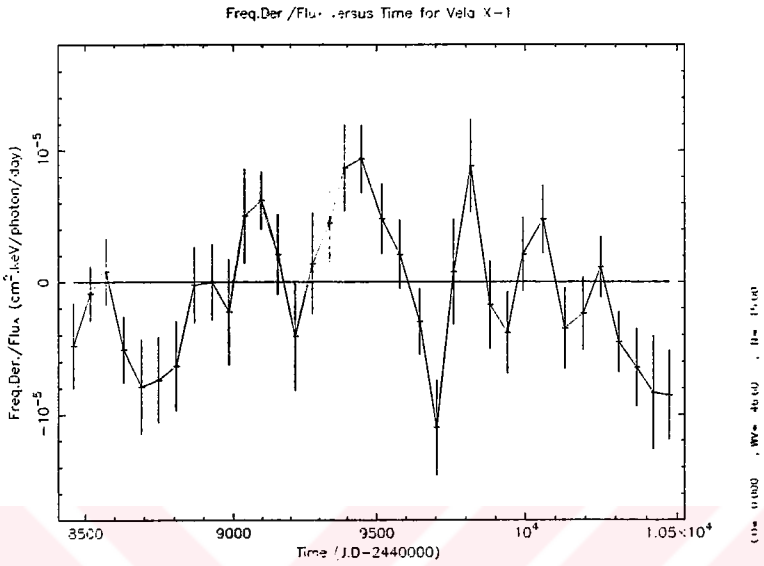

derivative suggests that we have short term disk reversals and continuously changing accretion geometry. In Figure (5.5), flux and frequency derivative over flux are seen to be uncorrelated. This shows that we do not have a correlation between flux and specific angular momentum. Evolution of specific angular momentum is presented in Figure (5.3). For 8928(J.D-2440000) and 9646(J.D-2440000), there are transitions from spin-down to spin-up with rapid increase in mass accretion rate (*see* Figures (5.2) and (5.1)). On these times, there is a change in accretion geometry: temporary accretion disk may be disrupted and flow may begin to be in radial direction increasing the mass accretion rate.

In conclusion for Vela X-1, we can say that the pulsar accretes mass via companion's stellar wind and temporary accretion disk formation is possible around

Figure 5.4: Flux versus Frequency Derivative for Vela X-1. Derivative of the frequency data and flux data were reduced by making bins each covering 45 days.

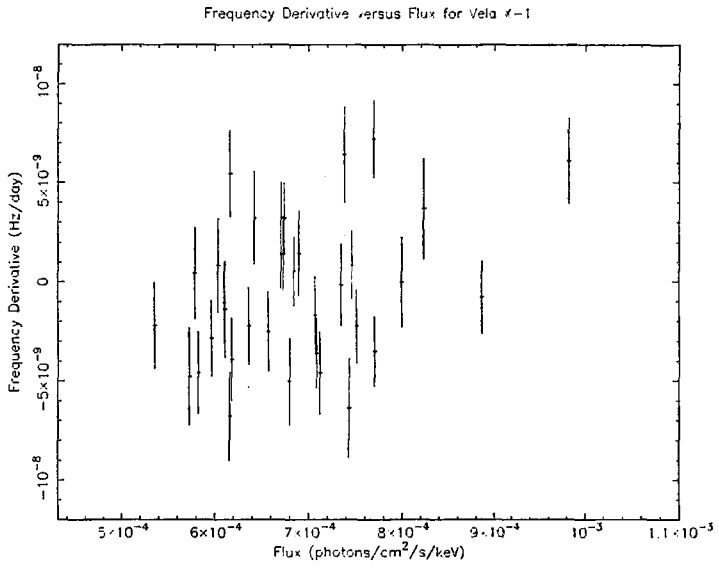

the pulsar.

5.2 GX 301-2

5.2.1 Properties

700s pulsations from GX 301-2 (4U 1223-62) were discovered by Ariel 5 in 1975 (White et al. 1976). GX 301-2 was, on average, neither spinning up nor spinning down between 1975 and 1985. After 1985, a spin-up period began with $\dot{\nu} \sim 10^{-9}$Hz.day^{-1} (Nagase 1989). Currently, pulsar spin period has reached $\sim 676s$. GX 301-2, being in a 41.5 day eccentric orbit ($e = 0.47$), is an accreting pulsar with the supergiant companion Wray 977 (Sato et al. 1986). This source

Figure 5.5: Flux versus frequency derivative over flux for Vela X-1. Data were reduced by making bins each covering 45 days.

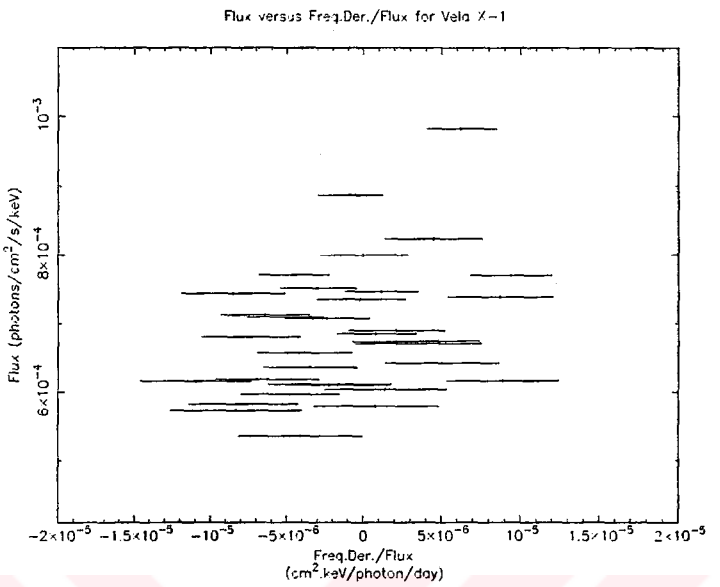

Figure 5.6: Frequency derivative versus frequency derivative over flux for Vela X-1. Data were reduced by making bins each covering 45 days.

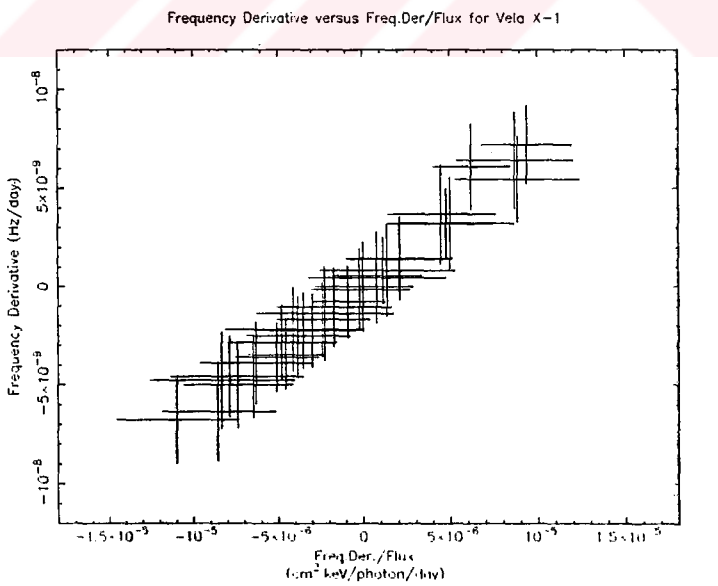

Figure 5.7: Flux and Frequency of GX 301-2 from the BATSE CONT data. Original data were reduced by making bins each covering 30 days.

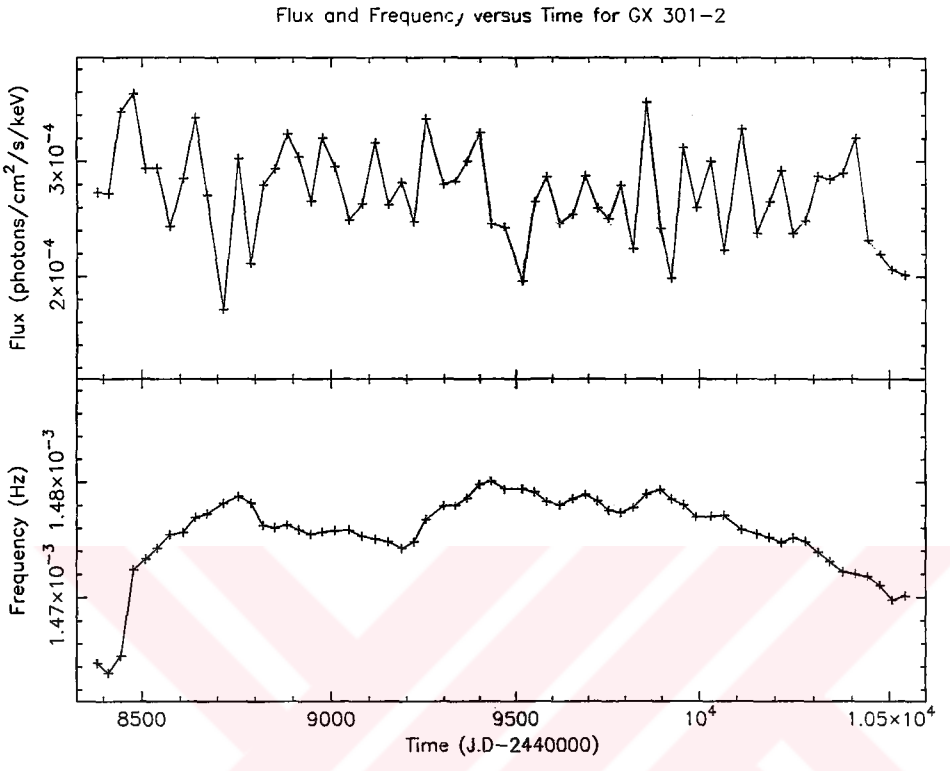

exhibited two rapid spin-up episodes at $\sim$ 8450 (J.D-2440000) and $\sim$ 9250 (J.D-2440000) which are also seen in Figure (5.7). These two spin-up episodes suggest the existence of long-lived ($\approx$ 30days) accretion disk (Koh et al. 1997).

5.2.2 Results

Frequency and X-ray flux data from GX 301-2 cover the interval between 8371 (J.D-2440000) and 10577 (J.D-2440000) (*See* Figure (5.7)). Data were reduced by making bins each covering 30 days. Average frequency on this interval is

Figure 5.8: Frequency derivative versus time for GX 301-2. Data were reduced by making bins each covering 30 days.

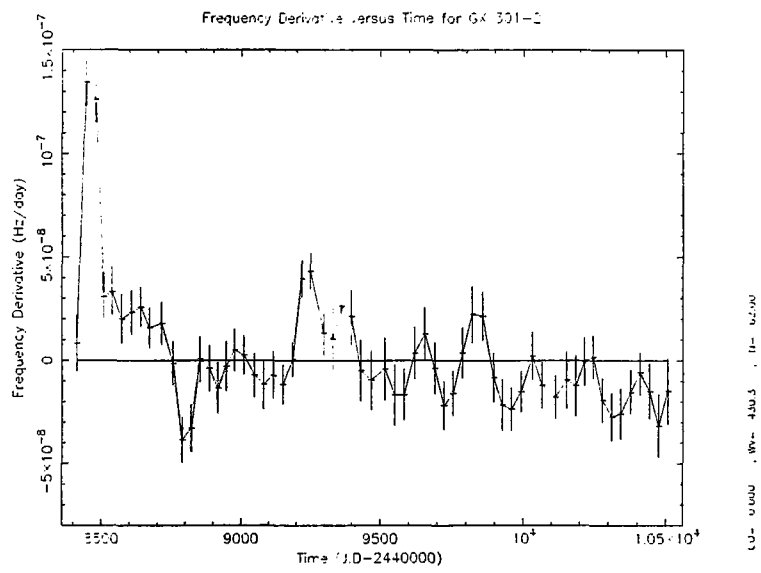

1.48×10^{-3}Hz, while average flux is 2.72×10^{-4}photons.cm^{-2}s^{-1}keV^{-1}.

From Figure (5.10), no correlation between flux and frequency derivative is seen which shows that the accretion is not via stable accretion disk. There is a correlation between frequency derivative over flux and frequency derivative which is equivalent to a correlation between specific angular momentum and torque. This correlation is valid for positive, negative and near zero values of frequency derivative showing that there are short term disk reversals and continuosly changing accretion geometry (*see* Figure (5.12)).In Figure (5.11), flux and frequency derivative over flux are seen to be uncorrelated. This shows that we do not have a correlation between flux and specific angular momentum. Evolution of specific angular momentum is presented in Figure (5.9). For 9186 (J.D-2440000) and

Figure 5.9: Frequency derivative over flux versus time for GX 301-2. Data were reduced by making bins each covering 30 days.

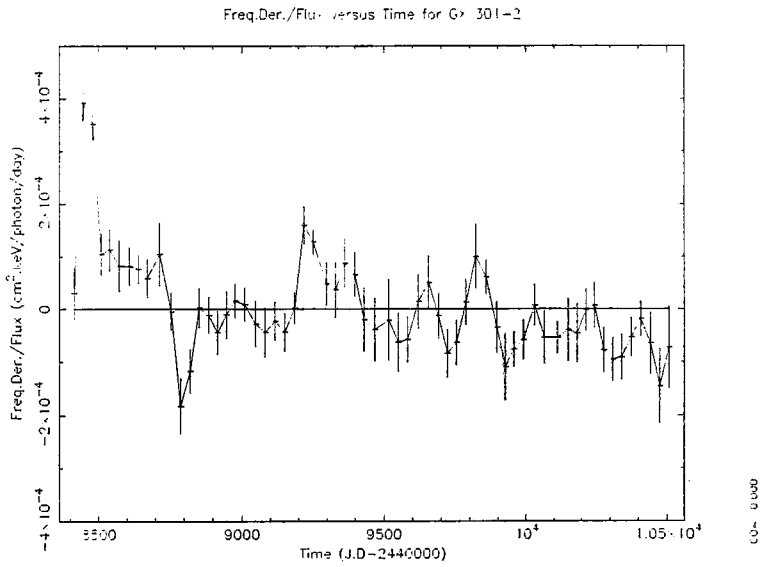

9787 (J.D-2440000), increase in mass accretion rate (as reflected by the increase in flux) is accompanied by the change in the sign of the frequency derivative(*see* Figures (5.7) and (5.8)). On these times, there is a change in accretion geometry: temporary accretion disk may be disrupted and flow may begin to be in radial direction increasing the mass accretion rate.

In conclusion for GX 301-2, we can say that the pulsar accretes mass from the companion's stellar wind and accretion from temporary accretion disks is possible for this source.

Figure 5.10: Flux versus frequency derivative for GX 301-2. Derivative of the frequency data and flux data were reduced by making bins each covering 30 days.

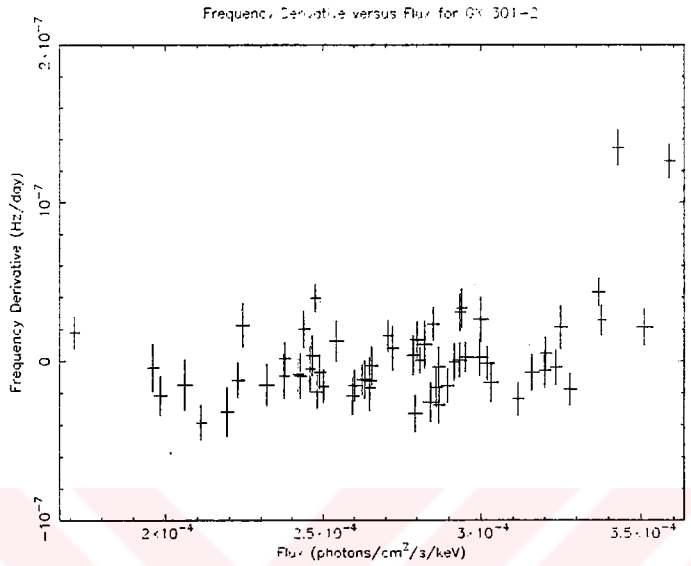

Figure 5.11: Flux versus frequency derivative over flux for GX 301-2. Data were reduced by making bins each covering 30 days.

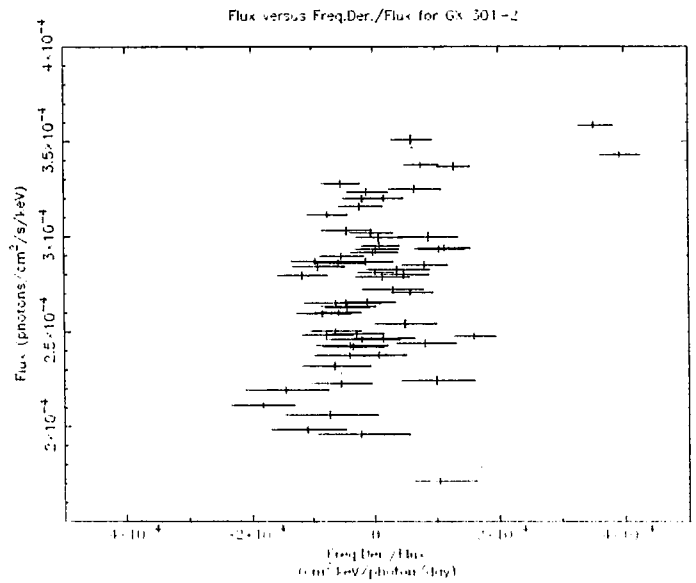

Figure 5.12: Frequency derivative versus frequency derivative over flux for GX 301-2. Data were reduced by making bins each covering 30 days.

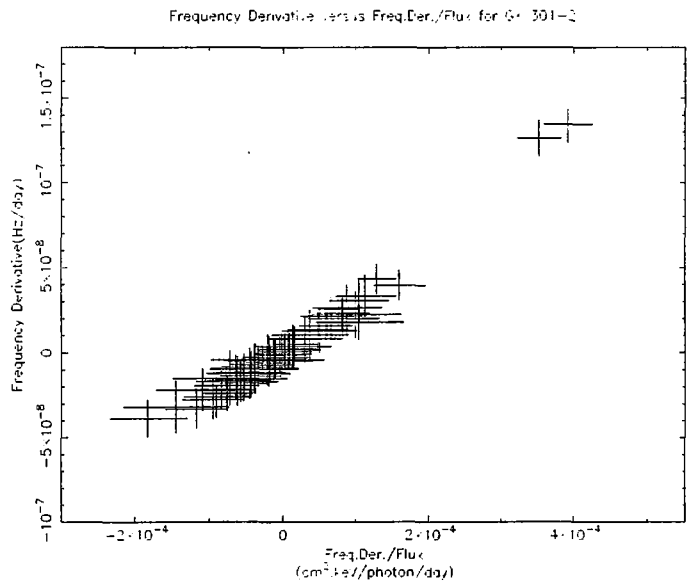

5.3 OAO 1657-415

5.3.1 Properties

38.22s pulsations from OAO 1657-415 were discovered in 1978 from HEAO 1 observations (White et al. 1979). The optical companion of OAO 1657-415 is probably a OB type star. Its binary orbit period was found to be 10.4 days from the eclipse due to its companion (Chakrabarty 1993).

5.3.2 Results

Frequency and X-ray flux data from OAO 1657-415 cover the interval between 8372 (J.D-2440000) and 10302 (J.D-2440000) (*See* Figure (5.13)). Data were reduced by making bins each covering 16 days. Average frequency on this interval

Figure 5.13: Flux and Frequency of OAO 1657-415 from the BATSE CONT data. Original data were reduced by making bins each covering 16 days.

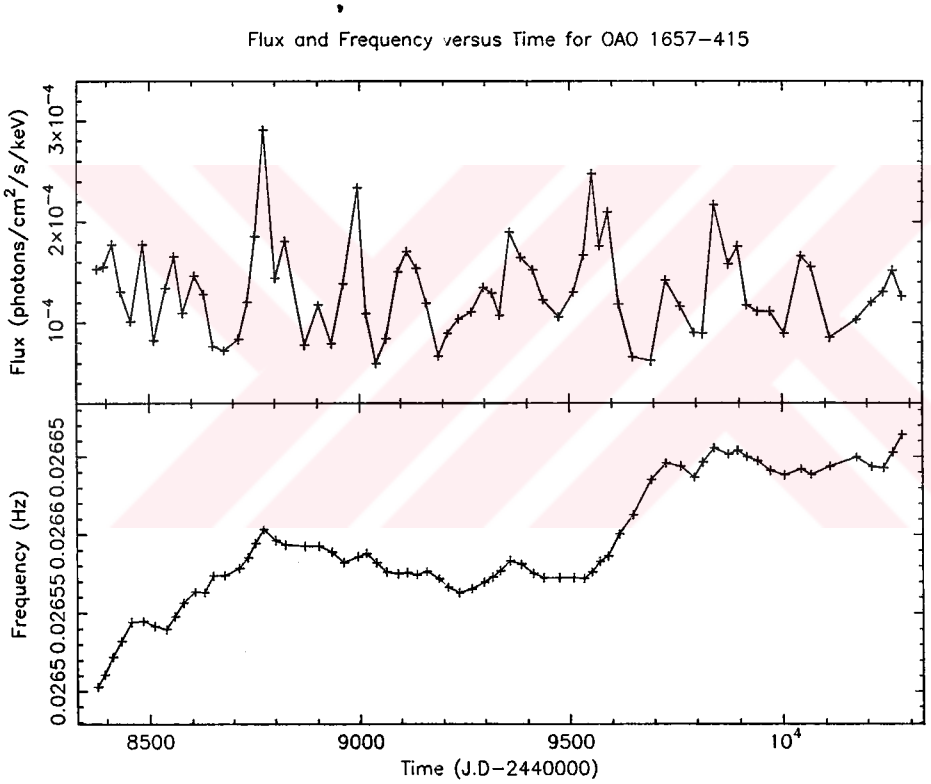

Figure 5.14: Frequency derivative versus time for OAO 1657-415. Data were reduced by making bins each covering 16 days.

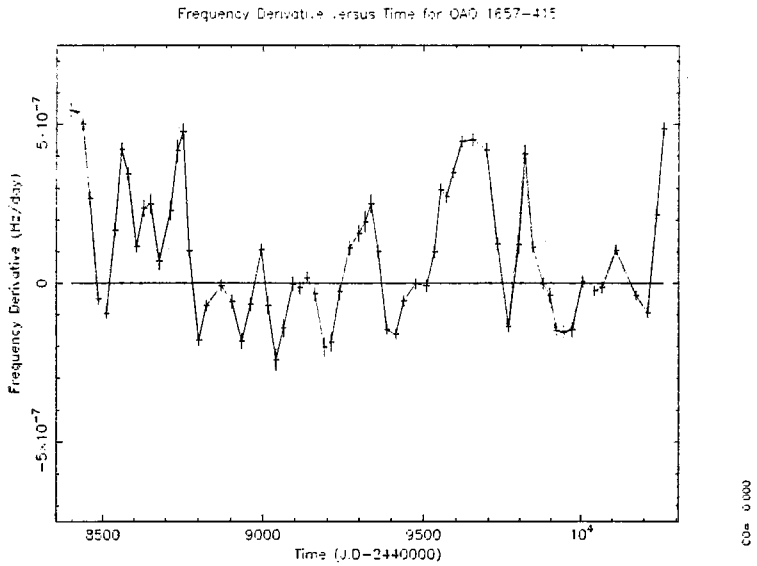

is 2.66×10^{-2}Hz, while average flux is 1.37×10^{-4}photons.cm^{-2}s^{-1}keV^{-1}.

There is no correlation between frequency derivative and flux (*see* Figure (5.16)). This suggests that there is no stable accretion disk formation for OAO 1657-415. From Figure (5.17), it is seen that we have both positive and negative specific angular momentum values for any flux range. It is also seen that the absolute value of the specific angular momentum decreses with flux. This may be an indication of formation of accretion disks with positive and negative sense of rotation since for Keplerian accretion disks we expect a weak dependence between specific angular momentum coming from the inner boundary of the disk and the X-ray luminosity ($l_k \propto L_x^{-1/7}$). However this dependence cannot explain the near zero values of specific angular momentum for high values of flux, so Figure (5.17)

Figure 5.15: Frequency derivative over flux versus time for OAO 1657-415. Data were reduced by making bins each covering 16 days.

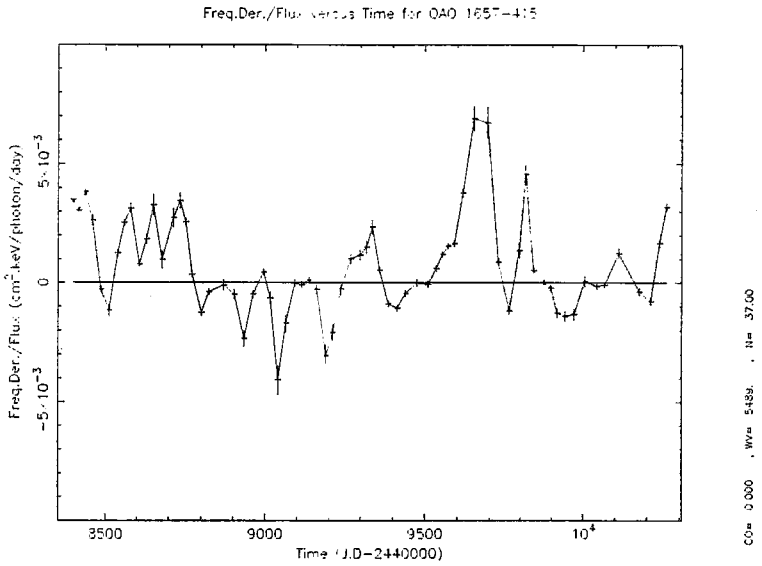

can be explained if we assume different accretion geometry with different flux values (i.e for low flux values prograde and retrograde disk formation is more likely to occur). From Figure (5.18), it is seen that there is a correlation between frequency derivative over flux and frequency derivative. Since frequency derivative over flux is directly proportional to the specific angular momentum carried by the accreted plasma, this correlation is equivalent to the correlation between frequency derivative and specific angular momentum. A correlation between frequency derivative and specific angular momentum for positive, negative and near zero values of frequency derivative shows us that we have short term disk reversals and continuously changing accretion geometry. For 9040(J.D-2440000), 9189(J.D-2440000), 9336(J.D-2440000), 9651(J.D-2440000), 9692(J.D-2440000),

and 10111(J.D-2440000), magnitude of specific angular momentum is high while mass accretion rate (which is indicated by flux) is low (*see* Figures (5.15) and (5.13)). High specific angular momentum and low mass accretion rate may be the indication an accretion disk. For various time values,[2] there are transitions from spin-down to spin-up with rapid increase in mass accretion rate (*see* Figures (5.14) and (5.13)). On these times, there is a change in accretion geometry: temporary accretion disk may be disrupted and flow may begin to be in radial direction increasing the mass accretion rate.

In conclusion for OAO 1657-415, we can say that the pulsar accretes mass from the companion's stellar wind with temporary prograde and retrograde accretion disk formation. When compared with Vela X-1 and GX 301-2, OAO 1657-415 shows an extra correlation -namely a correlation between the absolute value of specific angular momentum and flux-, which is an additional evidence for the temporary disk formation. Data used here is more recent than the one used before (Baykal, 1997), but similar results were obtained.

[2] $\simeq$ 8772,9114,9359,9553,9841,10043 (J.D-2440000)

Figure 5.16: Flux versus Frequency Derivative for OAO 1657-415. Derivative of the frequency data and flux data were reduced by making bins each covering 16 days.

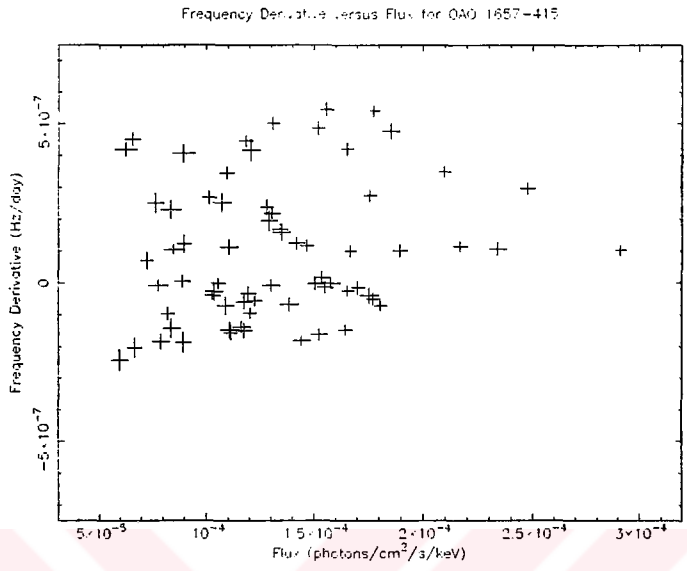

Figure 5.17: Flux versus frequency derivative over flux for OAO 1657-415. Data were reduced by making bins each covering 16 days.

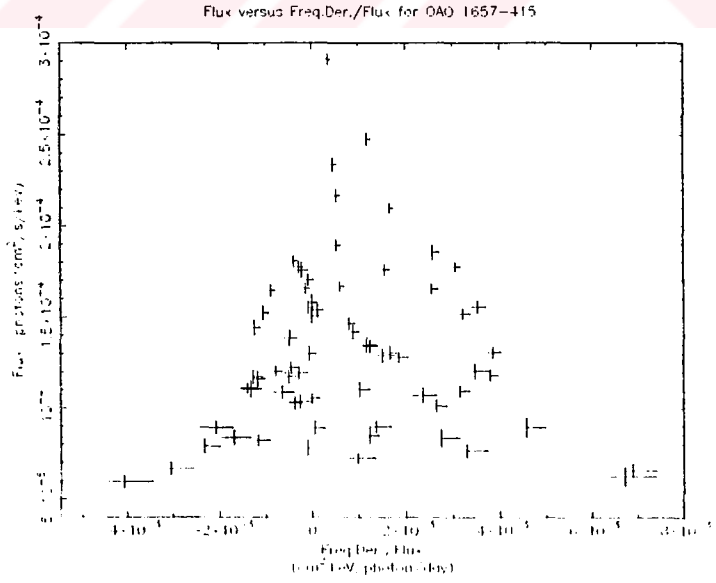

Figure 5.18: Frequency derivative versus frequency derivative over flux for OAO 1657-415. Data were reduced by making bins each covering 16 days.

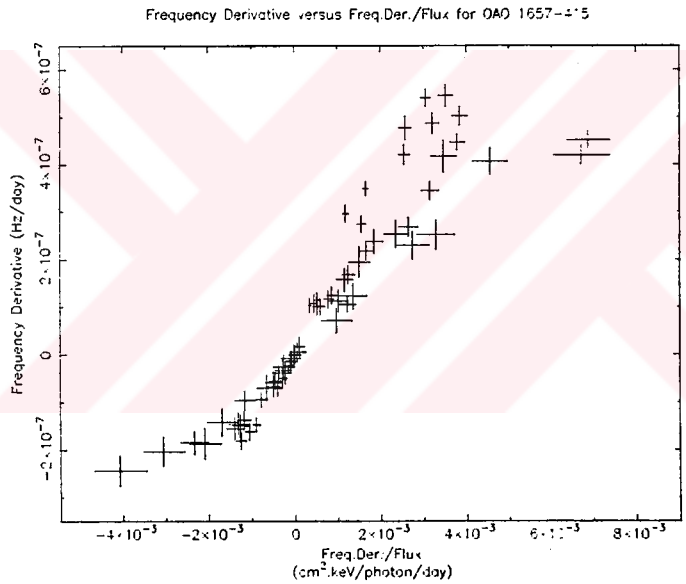

CHAPTER 6

BATSE OBSERVATIONS ON LOW MASS SYSTEMS

In this chapter, two low mass systems (GX 1+4 and 4U 1626-67) are discussed. These are thought to be accreting from accretion disks with lifetimes of $\simeq$ years.

6.1 GX 1+4

6.1.1 Properties

Among 10 X-ray pulsars, GX 1+4 is the only one that shows an anticorrelation between its frequency derivative and X-ray luminosity (between 8370 (J.D-2440000) and 9630 (J.D-2440000)) This anticorrelation was discussed before (Chakrabarty 1996,1997) . However, this anticorrelation is not seen between 9800 (J.D-2440000) and 10540 (J.D-2440000). Also, a positive correlation between frequency derivative and flux is found for the interval between 9640 (J.D-2440000) and 9760 (J.D-2440000) where spin-up is observed.

2 minute pulsations from GX 1+4 were discovered by an 18-50 keV X-ray balloon experiment in 1970 (Lewin et al. 1971) This source is a low mass X-ray binary with the optical companion being M6 III giant V2116 Oph (Chakrabarty & Roche 1997). GX 1+4 was spinning up rapidly with a mean rate $\sim 6.0 \times 10^{-12}$Hz/s in 1970s (Nagase 1989). After 1987, it reappeared with a spin-down

Figure 6.1: Flux and Frequency versus Time for GX 1+4. No binning was performed.

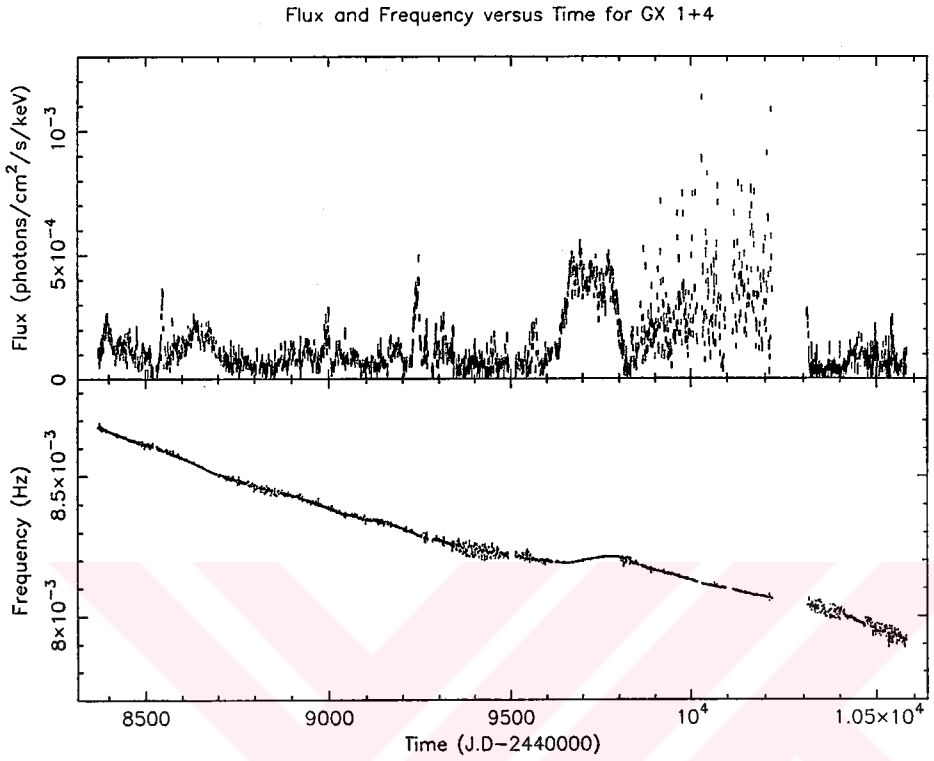

trend (Makishima et al. 1988).

6.1.2 Results

Frequency and X-ray flux data from GX 1+4 cover the interval between 8370 (J.D-2440000) and 10540 (J.D-2440000) (*See* Figure (6.1). Data between 8370 (J.D-2440000) and 9630 (J.D-2440000) were reduced by making bins each covering 60 days. On this interval, the average flux is 1.11×10^{-4}photons.cm^{-2}s^{-1}keV^{-1} and average period is 118.1s. There is a continuous spin-down with a rate 8.41 ×

T.C. YÜKSEKÖĞRETİM KURULU
DOKÜMANTASYON

Figure 6.2: Frequency Derivative versus Flux for GX 1+4 between 8370 (J.D-2440000) and 9630 (J.D-2440000). Data were reduced by making bins each covering 60 days.

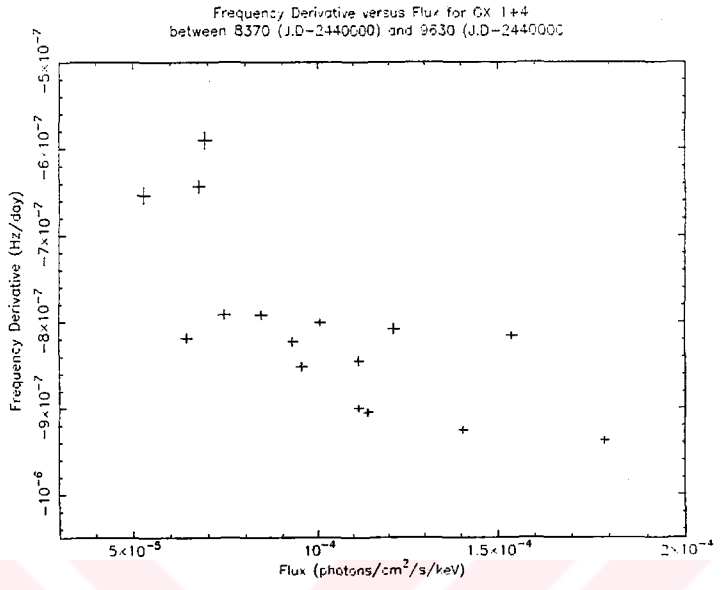

10^{-7}Hz.day^{-1} on this interval and it is found that there exists an anticorrelation between the frequency derivative and flux (*See* Figure (6.2), and also Chakrabarty 1996,1997)).

Between $\simeq$ 9650 (J.D-2440000) and $\simeq$ 9800 (J.D-2440000), the source spins-up with a rate 1.89 $\times$ 10^{-7}Hz/day. On this interval, flux increases,too ($\simeq$ 4 $\times$ 10^{-4}photons.cm^{-2}s^{-1}keV^{-1}). Between 9640 (J.D-2440000) and 9760 (J.D-2440000), a positive correlation between flux and frequency derivative is found (*See* Figure (6.3)).

Between 9800(J.D-2440000) and 10300(J.D-2440000), the source is again in spin-down phase with a spin-down rate of 3.21 $\times$ 10^{-7}Hz/day. For this interval, no correlation is seen between frequency derivative and flux (*See* Figure (6.4)).

Figure 6.3: Frequency Derivative versus Flux for GX 1+4 between 9640 (J.D-2440000) and 9760 (J.D-2440000). Data were reduced by making bins each covering 20 days.

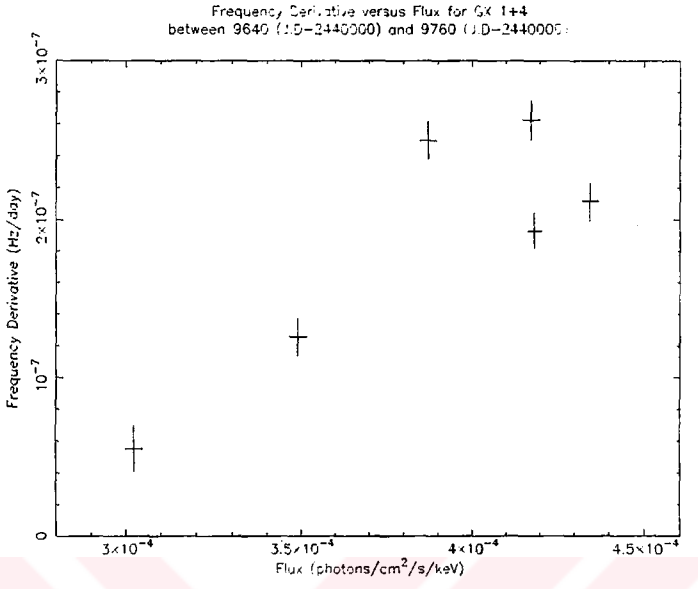

Figure 6.4: Frequency Derivative versus Flux for GX 1+4 between 9800 (J.D-2440000) and 10300 (J.D-2440000). Data were reduced by making bins each covering 10 days.

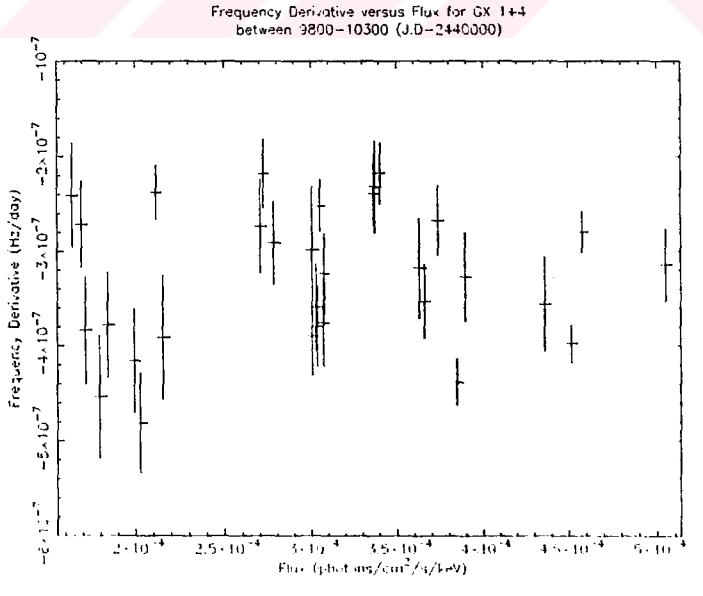

Figure 6.5: Flux versus Frequency Derivative for GX 1+4 between 10300 (J.D-2440000) and 10540 (J.D-2440000). Data were reduced by making bins each covering 10 days.

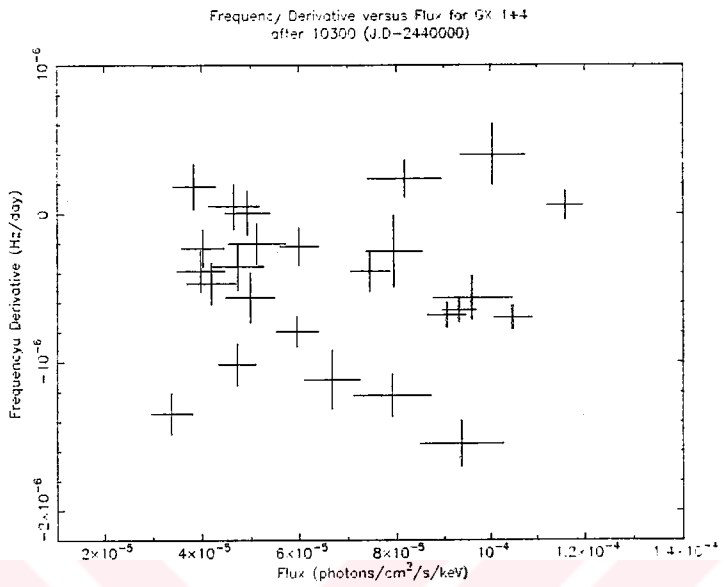

On this interval, flux fluctuates considerably (*See* Figure (6.1)).

Between 10300(J.D-2440000) and 10540(J.D-2440000), the source is again in spin-down phase with a spin-down rate of 5.01×10^{-7}Hz/day. For this interval, no correlation is seen between frequency derivative and flux (*See* Figure (6.4)). On this interval, fluctuations in flux are less than the previous interval (*See* Figure (6.1)).

Spin-down with negative correlation between frequency derivative and flux may be considered as an indication of the presence of a stable retrograde Keplerian accretion disk which is formed by Roche-lobe overflow (Nelson et. al. 1997). However, if GX 1+4 is a system undergoing Roche-lobe overflow, then there is no known mechanism that can explain the presence of a retrograde accretion

disk with a lifetime being of the order of years (Nelson et al. 1997). Nelson et al. (1997) suggest that the disk may be fed by X-ray excited wind instead of Roche-lobe overflow. Early studies about the disk formation in wind-accreting pulsars demonstrate that it may be possible to form temporary accretion disks with alternating senses of rotation in these systems (Matsuda et al. 1987,1991 , Fryxell & Taam 1988,1989, Blondin et al. 1990). Typical lifetime for such a disk formation is about the sound crossing time of the accretion radius, which is of the order of hours for the neutron star accreting from a fast wind originating from an early type (O or Be) star. This timescale is not applicable to GX 1+4, since its companion is a red giant and has a very wide orbit (Chakrabarty & Roche 1997, Murray et al. 1998). A timescale of the order of years for a prograde or a retrograde disk is plausible (Murray et al. 1998). There are also other explanations for the spin-down with anticorrelation with the frequency derivative if we assume the accretion to be due to Roche lobe overflow of the companion star. Yi et al. (1997) suggest that this spin-down may be due to a radially advective sub-Keplerian accretion disk. This explanation requires a critical $\dot{M}$ of $\sim 10^{16}\mathrm{g.s}^{-1}$, but observations imply a much higher rate($\sim 10^{17} - 10^{18}\mathrm{g.s}^{-1}$)(Nagase 1989; Nelson et.al. 1997). Kerkwijk et al. (1998) state that such spin-down trends in accretion powered pulsars can be explained by the tilt of the inner region of the disk by more than 90 degrees, i.e inner disk behaves like a retrograde disk. Their simulation shows the possibility of the disk tilt, but they do not suggest a mechanism that would reset the system and return original prograde configuration.

Positive correlation between flux and frequency derivative in the spin-up region

(*See* Figure (6.3)) is very interesting, since it is a sign of a prograde accretion disk. For this interval, we can say that there is a possibility of prograde accretion disk formation using Equation (3.33).

For intervals between 9800 (J.D-2440000) - 10300 (J.D-2440000) and 10300 (J.D-2440000) - 10540 (J.D-2440000), continuous spin-down is observed but correlation between frequency derivative and flux disappears. On these intervals, either the bolometric X-ray flux is uncorrelated with the torque which may indicate the change of accretion geometry or the X-ray flux coming from 20-50 keV band does not have the same trend with the bolometric X-ray flux. If the latter possibility is the case, it implies a change in the X-ray spectrum.

6.2 4U 1626-67

6.2.1 Properties

Pulsations with the period $\sim$ 7.7s from 4U 1626-67 were discovered in 1977 during SAS 3 observations (Rappaport et al. 1977). The optical counterpart of 4U 1626-67 was found to be KZ Tr A which is an extremely low mass star with the mass $\sim 0.02 - 0.06 M_{\odot}$ (Chakrabarty 1997). Upper limit for the projected semimajor axis of the binary orbit ($a \sin i$) was found to be $< 10 lt - ms$ (Levine et al. 1988) which makes accretion due to Roche-lobe overflow probable. Orbital period of 4U 1626-67 was found to be $\sim$ 2485s (Middleditch et al. 1981).

Figure 6.6: Flux and Frequency versus Time for 4U 1626-67. 90 day binning in data were made.

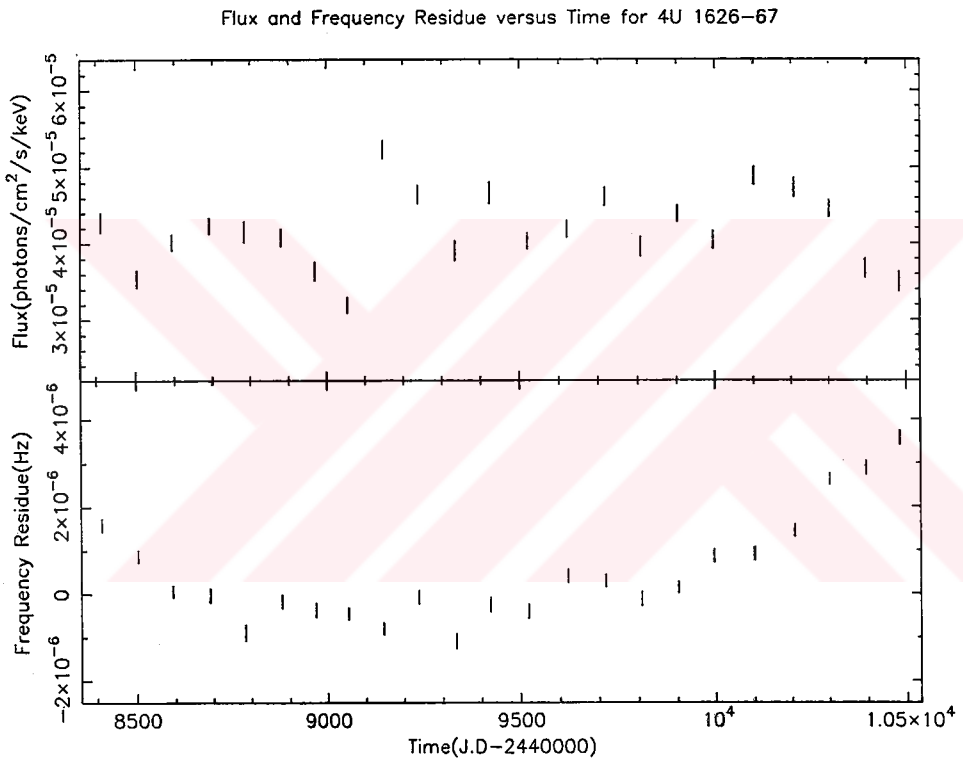

Figure 6.7: Frequency derivative versus flux for 4U 1626-67. Original data were reduced by making bins each covering 90 days.

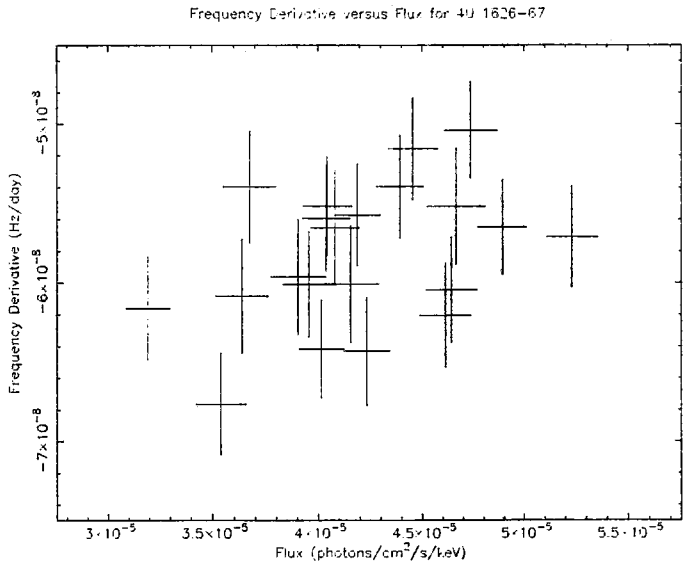

6.2.2 Results

Frequency and X-ray flux data from 4U 1626-67 cover the interval between 8371 (J.D-2440000) and 10580 (J.D-2440000) (*See* Figure (6.6)). Average frequency on this interval is 0.13 Hz and average flux is 4.16×10^{-5}photons.cm^{-2}s^{-1}keV^{-1}. This source shows an overall spin-down with a rate of 5.92×10^{-8}Hz.day^{-1} with the frequency residues plotted in Figure (6.6).

From Figure (6.7), we see a correlation between frequency derivative and flux. This is equivalent to an anti-correlation between absolute value of the frequency derivative and flux. This may be an indication of a prograde Keplerian disk with a large fastness parameter which is defined in Equation (3.23). In other words, there may exist a prograde accretion disk with the spin-down magnetic torques

dominated (N_2 defined in Equation (3.20)), so that we have a net torque in the opposite sense of rotation.

CHAPTER 7

CONCLUSION

In this thesis, analysis of BATSE X-ray flux and frequency data for 10 accretion powered pulsars (GX 1+4, 2S 1417-624, GS 0834-430, 4U 1626-67, Vela X-1, OAO 1657-415, GX 301-2, A 1118-616, GRO J1948+32, GRO J1008-57) are presented.

2 of these sources (GS 0834-430 and 2S 1417-624) are found to be torque and X-ray luminosity correlated. Both 2S 1417-624 and GS 0834-430 are transient pulsars and correlation of torque and X-ray luminosity for these 2 pulsars may imply the existence of prograde Keplerian accretion disks. But, since these two pulsars are not persistent sources, this may show that accretion disks form from companions' strong winds or temporary Roche lobe overflow in the vicinity of their periastron epochs. For these two sources, α in the relation $\dot{\Omega} \propto L^{\alpha}$ is greater than 1 within 1σ error limits. Within 2σ, on the other hand, differentiating a unique inner disk model is not possible. For 2S 1417-624, the spectral model considered is found to be lacking to explain the observed high frequency derivative. For GS 0834-430, 1T Opt Opt Thick RPD, and 2T Opt Thin GPD Compt brems, and Ghosh-Lamb models are possible within 2σ, but it is impossible to differentiate a single model among them.

For 3 of the 10 sources (Vela X-1, GX 301-2, OAO 1657-415) which are thought

to be accreting from wind, we investigate the possibility of temporary accretion disk formation. We found that there is a continous change in accretion geometry and temporary accretion disk formation is possible for these sources.

For GX 1+4, an anti-correlation between spin frequency derivative and flux is found for the first part of the data interval in which continous spin-down is observed. This anti-correlation shows a correlation between X-ray luminosity and torque exerted on the opposite sense with the spin direction of the neutron star. This anti-correlation may be the indication of a retrograde disk formation (Nelson et al. 1997), a radially advective sub-Keplerian accretion disk (Yi et al. 1997) or a warped accretion disk (van Kerkwijk et al. 1998). In the second interval, GX 1+4 shows a spin-up state which was not discussed before. It is interesting to find a correlation of torque and X-ray luminosity for this interval which is a strong indication of a prograde disk formation. In the third and the forurth intervals, there is again a continuous spin-down like the first interval, but no correlation is found between torque and X-ray luminosity. On these intervals, either the bolometric X-ray flux is uncorrelated with the torque which may indicate the change of accretion geometry or the X-ray flux coming from 20-50 keV band does not have the same trend with the bolometric X-ray flux. If the latter possibility is the case, there should be a change in the X-ray spectrum.

For 4U 1626-67, a correlation between X-ray luminosity and torque is found. This correlation may be a sign of a prograde disk. Since we have a net spin-down torque, fastness parameter should be high ($\omega_s > \omega_c \sim 0.35$).

It is important to note that our flux data were in the 20-50 keV band. For

our analysis, we assumed that the trend of the flux on this band is similar to the bolometric X-ray flux. A new instrument that is capable of detecting the flux coming from a broader range including soft X-ray range will be useful for future studies.

REFERENCES

[1] Anzer, U., Börner G. 1980, A&A, 83,133

[2] Aoki et al. 1992, PASJ, 44, 641

[3] Apparao, K.M.V. et al. 1980, A&A, 89,249

[4] Baykal, A. 1997, A&A, 319,515

[5] Bildsten L. et al. 1997, ApJS, 113,367

[6] Blondin, J.M. et al. 1990, ApJ, 356, 591

[7] Chakrabarty, D. 1993, ApJ, 403, L33

[8] Chakrabarty, D. 1996, Ph.D Thesis submitted to California Institute of Technology

[9] Chakrabarty, D. 1997, ApJ, 481, L101

[10] Chakrabarty, D., Roche, P. 1997, ApJ, 489, 254

[11] Coe, M.J. et al. 1994a, A&A, 289, 784

[12] Coe, M.J. et al. 1994b, MNRAS, 270, L57

[13] Corbet, R.H.D. 1986, MNRAS, 220, 1047

[14] Davidson, K., Ostriker, J.P. 1973, ApJ, 179, 585

[15] Davies, R.E., Fabian A.C, Pringle J.E. 1979, MNRAS, 186, 779

[16] Elsner, R.F., Lamb, F.K., 1977, ApJ, 215,897

[17] Eyles, C.J. 1975, Nature, 254, 577

[18] Finger et al. 1996, A&A SS, 120, 209

[19] Ghosh, P., Lamb, F.K. 1978, ApJ, 223, L83

[20] Ghosh P., Lamb, F.K. 1979a, ApJ, 232, 259

[21] Ghosh P., Lamb, F.K. 1979b, ApJ, 234, 296

[22] Ghosh, P., Lamb, F.K. 1991, from Neutron Stars: Theory and Observation, Kluwer Academic Publishers, eds. J.Ventura, D.Pines, 1991, pp.363-444

[23] Ghosh, P., Lamb, F.K. 1992, X-Ray Binaries and Recycled Pulsars, eds. E.P.J. van den Heuvel and S.A. Rappaport, 487-510

[24] Grindlay, J.E. et al. 1984, ApJ, 276, 621

[25] Heinze, K.G. 1976, ApJS, 30, 491

[26] Illarionov, A.F., Sunyaev, R.A. 1975, A&A, 39, 185

[27] Ives J.C. et al. 1975, Nature, 254, 580

[28] Giacconi, R. et al. 1971, ApJ, 167, L67

[29] Kelley, R.L. et al. 1981, ApJ, 243, 251

[30] King, A. 1995, from X-ray binaries, Cambridge University Press, eds. W.H.G.Levin, J. van Paradijs, E.P.J. van den Heuvel.

[31] Lamb, F.K. et al. 1973, ApJ, 184,271

[32] Levine, A. et al. 1988, ApJ, 327, 732

[33] Lewin, W.H.G. et al. 1971, ApJ, 169, L17

[34] Lipunov, V.M. 1992, "Astrophysics of Neutron Stars," Springer-Verlag

[35] Lipunov, V.M. 1987, Astrophys. Space Sci., 132, 1

[36] Makishima, K. et al. 1988, Nature, 333, 746

[37] Matsuda, T. et al. 1991, ApJ, 248, 301

[38] McClintock, J.E. et al. 1976, ApJ, 206, L99

[39] Middleditch, J. et al. 1981, ApJ, 244, 1001

[40] Mineshige, S. et al. 1991, MNRAS, 251, 555

[41] Murray, J.R. et al. 1998, astro-ph 9810118

[42] Nagase, F. 1989, PASJ, 41, 1

[43] Nelson, R.W. et al. 1997, 488, L117

[44] Pringle, J.E., Rees M.J., 1972, A&A, 21, 1

[45] Rappaport, S. et al. 1976, ApJ, 206, L103

[46] Rappaport, S. et al. 1977, ApJ, 217, L29

[47] Schreier, E. et al. 1972, ApJ, 172, L79

[48] Shakura, N.I, Sunyaev, R.A. 1973, A& A, 24, 337

[49] Shapiro, S.L. et al. 1976, ApJ, 204, 187

[50] Stollberg, M.T. et al. 1993, IAU Circ No. 5836

[51] Taam, R.E., Fryxell, B.A., 1988a, ApJ, 327, L73

[52] Taam, R.E., Fryxell, B.A., 1988b, ApJ, 335, 862

[53] Taam, R.E., Fryxell, B.A., 1989, ApJ, 339, 297

[54] van Kerkwijk, M.H. et al. 1998, astro-ph 9802162

[55] Vidal, N.V. et al. 1973, ApJ, 265, 1036

[56] Waters, L.B.F.M., van Kerkwijk, M.H. 1989, A& A,223, 196

[57] White, N.E. et al. 1993, X-Ray Binaries, eds. W.H.G.Lewin et al., 1-57

[58] Yi, I. et al. 1997, ApJ, 481, L51